Review

Role of MXenes/Polyaniline Nanocomposites in Fabricating Innovative Supercapacitor Technology

Dipanwita Majumdar [iD]

Department of Chemistry, Chandernagore College, Hooghly, WB, 712136, India
E-mail: wbesdmajumdar@gmail.com

Abstract: Versatile and exclusive electronic, optical, physicochemical, electrochemical and mechanical features of both conducting polymers and MXenes have stimulated global scientists to take serious impetuses in designing innovative high-performance energy storage systems with these materials, for resolving the growing needs for auto-powering mechanically flexible and wearable electronics for all essential technological fields. However, both the materials have experienced some serious practical limitations, which have driven the scientific community to look for necessary modifications in the form of MXenes/PANI nanocomposites with suitable compositions that would essentially restore their representative characteristics but successfully suppress their functional drawbacks concurrently and considerably. Accordingly, in the present overview, the different strategies of fabrication of MXenes/PANI nanocomposites for advanced supercapacitors with special reference to the necessary morphological modifications brought about by synthetic improvisations that resulted in superior capacitive, electronic charge transport as well as structural properties have also been recognized and compared. Such analysis would purposefully assist in adjusting the integral mechanical and electrochemical responses for scheming smarter and highly flexible microelectronics soon.

Keywords: MXenes, conducting polymers, polyaniline, nanostructures, composites, supercapacitors, flexible electronics, energy storage

1. Introduction

1.1 *Fundamentals of supercapacitor technology*

Appropriate management of fast fossil fuel exhaustion as well as environment pollution issues have been the main goal for worldwide scientists and engineers, who have devoted themselves to searching for novel and upgraded renewable and sustainable energy technologies in recent years [1-2]. To address this challenge, the electrochemical capacitors, also popularly known as supercapacitors or ultracapacitors, have made promotable contributions, especially, to administer the sky-high demands of energy backup devices for supporting not only regular but also heavy and sophisticated technologies in the fields of biomedical, astronomical and military engineering purposes that urge diligent as well as high-performing electronics with extraordinary robustness and mechanical flexibility [3].

Commonly, the electrochemical performance of ultracapacitors is dictated by two vital parameters, i.e., energy density (E) and power density (P) as specified by the equations (1) and (2) [4].

$$E = \int CdV = \frac{1}{2}CV^2 \qquad (1)$$

$$P = \frac{E}{t} \qquad (2)$$

In the above equation, C indicates the cell gravimetric/areal/volumetric capacitance, V represents operational voltage range, and t is the device discharging time period, respectively. The energy density (E) is one of the primary factors that dominate the proficiency of energy storage devices, thus, the desired standards can be well accomplished through the optimization of electrode capacitance output as well as expanding the working potential window of the device [5]. Currently, the commercialized ultracapacitors have low energy and power densities that originate from inferior electronic and morphological features of the fabricating materials and also often do not support long-term cycling stability during fast redox processes. Furthermore, their high structural stiffness and non-stretchability severely restrict their usage in devising flexible electronics. Nonetheless, all these challenges can be efficiently adjusted through appropriate selection and scheming of electroactive materials via tailoring of the chemical constitution, composition, geometrical and crystal parameters, microscopic adaptations, porosity, surface area, conductivity, wettability, etc. [6]. Therefore, wide-ranging researches are incessantly underflow for designing smarter electrode materials with exclusive multifunctional features to be used in self-powering devices like consumer displays, smart garments, and health monitors and allied systems. This has led to systematic and periodic evaluations in the form of high-quality reviews that equitably highlight their achievements as well as practical constraints [7-8].

1.2 *Polyaniline as superior electrode material for supercapacitors*

It has been widely accepted that pseudocapacitive materials result in boosted capacitive responses [8]. This realization has enormously promoted researches in designing various types of organic as well as inorganic-based pseudocapacitive nanomaterials. Thus, electrochemical explorations of various kinds of conducting polymer achieved a high degree of popularization owing to easy and low-costing preparatory advantages and attractive electrochemical responses.

Among the various widely available pseudocapacitive materials, the p-type conjugated polymer, polyaniline (PANI), has been broadly explored for electrochemical charge storage applications because of its high theoretical capacity (294 mAhg^{-1}, by assuming full doping and neglecting the mass of the anion), decent electrical conductivity, simplistic synthesis procedures and ease availability of raw materials. It shows the existence of several oxidation states, which has been consequently named as: the fully reduced form, called leuco-emeraldine (LE) (y = 1), the semi-oxidized form, commonly known as the emeraldine base (EB) (y = 0.5) and the fully oxidized form is named as pernigraniline (PE) (y = 0) respectively, as indicated schematically in Figure 1 [9].
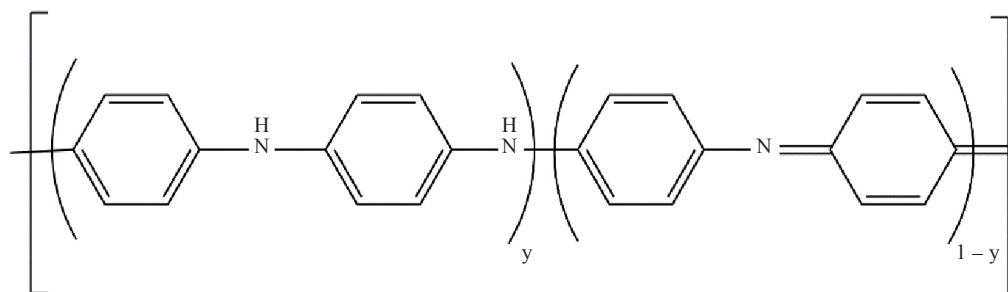
Figure 1. Chemical structure of PANI indicating different oxidation states: fully-reduced leuco-emeraldine (LE) state (y = 1), semi-oxidized emeraldine base (EB) state (y = 0.5) and fully-oxidized pernigraniline (PE) state (y = 0).

The excellent tunability of electrical conductivity in the doped-conjugated polymers such as polyanilines, polypyrroles, etc., was foremost reported through the revolutionary contributions made by the Heeger group [10], and accordingly was awarded the most prestigious Nobel Prize in Chemistry in the year 2000 for this noble discovery.

Different research groups in subsequent times reported the probable contribution of capacitive current in the electrochemistry of conducting polymers, which was further supported by cyclic voltammetry, galvanostatic charging/ discharging and electrochemical impedance spectroscopic investigations [11-12]. Even the pseudocapacitive behavior of PANI was reported in the pioneering works of Conway group followed by Arbizzani and coworkers and by Kaner and co-researchers while demonstrating the fundamental charge storage mechanisms in supercapacitors originating from Faradaic capacitive processes. They experimentally disclosed that PANI is naturally a pseudocapacitor material rather than a typical battery material [13-14].

In a short while, the Rudge group examined the doping influence of PANI on its charge storage responses, as indicated in Table 1, realizing that the capacitive behavior depends on the dopant's nature as well as doping extent, although the dependency behavior was non-linear [15].

Table 1. Effect of dopants on electrochemical performance of PANI

PANI dopants	Capacitance	Operating potential window	Electrolyte	% Capacitance retention (number of cycles)	References
PANI-HCl	70 Fg^{-1} @ current density of 1.25 mAcm^{-2}	0-1.0 V	1M Et$_4$NBF$_4$	57% (1000)	[16]
PANI-LiPF$_6$	115 Fg^{-1} @ current density of 3.75 Ag^{-1}	0-0.75V	1 M Et$_4$NBF$_4$	78% (5000)	[17]
Sulfonated PANI	1107 Fg^{-1} @ current density of 1 Ag^{-1}	0-1.2V	1 M H$_2$SO$_4$	-	[18]
De-doped PANI nanofibers	593 Fg^{-1} @ current density of 2.5 Ag^{-1}	0-0.65V	1 M H$_2$SO$_4$	70% (5000)	[19]

Table 2. Electrochemical performances of PANI nanostructures prepared via different synthesis methods

Pure PANI morphology	Synthesis technique	Specific capacitance	Capacitance retention % (number of cycles)	References
Nanotubes	Self-assembly	625 Fg^{-1} @ current density of 1Ag^{-1}	77% (500)	[20]
Nanotubes Nanospheres Nanofibers	Sacrificial template synthesis	477 Fg^{-1} 315 Fg^{-1} 385 Fg^{-1} @ current density of 1Ag^{-1}	66% (5000) 58% (5000) 61% (5000)	[21]
Nanorods	Self-assembly	455 Fg^{-1} @ voltage scan rate of 1mVs^{-1}	65% (1300)	[22]
Nanoworms	Self-assembly	301 Fg^{-1} @ current density of 0.5 Ag^{-1}	72.4% (1000)	[23]
Nanofiber	Electro-spinning	308 Fg^{-1} @ current density of 0.5Ag^{-1}	70% (1000)	[24]
Nanofibers	Interfacial polymerization	554 Fg^{-1} @ current density of 1Ag^{-1}	10% (1000)	[25]
Cross-linked nanoporous	Electrochemical polymerization	410 ± 5 Fg^{-1} @ voltage scan rate of 3 mVs^{-1}	100% (1000)	[26]

The probable cause might be due to the covalent attachment of some dopants to the PANI chains that do not undergo easy electrochemical exchange, thus inhibit a few proportions of PANI fragments towards capacitive functioning. The de-doping process induces morphological modifications that endorse better ion accessibility of

the electroactive material and generate capacitive enhancement. Hence, in this case, charge storage occurs via pseudocapacitive doping/de-doping processes causing anions to migrate in/out of the electrode and causing PANI to get oxidized or reduced subsequently. Accordingly, smooth mass transport of the dopant ion is an important issue, especially for highly dense PANI film electrodes. So scientists have taken the bold step of switching over to nanophase which can obviously display promising signatures owing to their highly porous and larger exposed surface advantages.

Thus, several facile synthetic strategies have been applied to obtain and optimize various morphology PANI nanostructures profitably and have demonstrated noticeable influence on the specific capacitance and cyclability performances with changing morphologies, as illustrated in Table 2.

A few years ago, Li et al. [27], reported maximum theoretical gravimetric capacitance for PANI of ~ 2000 Fg^{-1}, although the experimental values to date accomplished have been much inferior. One of the several causes that have been conferred is due to very small effective capacitive contributions from PANI chains, which is again guided by its electrical conductivity as well as morphology that controls the extent of diffusion of ions embracing it. In a typical study of controlling nanostructure porosities, it got proved that the capacitance could be doubled just by modifying the structural features simply via varying synthetic procedures [28].

Although several comprehensive investigations have been carried out with pristine PANI nanoforms for supercapacitor research, their overall electrochemical performances have been relatively inferior to meet commercial necessities primarily due to their extremely poor electrochemical stability during repetitive charging/discharging cycles. These systems undergo structural swelling and abrupt polymer backbone shrinking induced by non-stop ion intercalation/de-intercalation actions during tedious charging/discharging processes leading to rapid and large capacitance fall. Further, their low solubilities in common solvents severely restrict in easy film deposition and processing needed for preparing much demanded planar semiconductor technology [29]. Hence, researchers have opted for various PANI-based nanocomposites through an appropriate blending of PANI with suitable materials for the purpose of improving the processibility, scalability and reproducibility besides modifying the morphology as well as electronic characteristics in order to accomplish superior and sustainable electrochemical behavior for advanced supercapacitor applications [30].

In recent years, exhaustive studies have reflected that the conducting polymer-based composite electrodes undoubtedly confirm considerable improvement in the electrochemical performance owing to the following reasons: i) firstly, the enhanced extent of surface functional groups modifications escalates the electroactive sites availability for Faradaic electron exchange processes as well as favors better compact holding of the electroactive components at the nanoscale dimensions, thereby preventing mutual aggregation issues. Also increase in functional moieties promoted the hydrophilic character, which is much needed for solution dispersing purposes for film preparation. ii) The flexible conducting polymer chains in the composites ensure decent interfacial contacts between the active components to ensure ultrafast charge transportation kinetics, very much commended for capacitance upgradation. iii) Composite formation also prevents unwanted mechanical deformation of the conducting polymer chains, ensuring structural tenacity for enduring large charging/discharging cycles, thereby promoting better electrochemical stability [31]. Thus, it has been a tedious job for the worldwide scientific community to search and choose appropriate components for fabricating desired conducting polymer-based nanomaterials for framing highly efficient energy storage systems.

1.3 *How good are MXenes as auxiliary electrode materials?*

Rigorous surveys in materials science have manifested the use of tailorable two-dimensional layered materials for innovative energy storage utilities [32-33]. They are bestowed with advanced mechanical along with tunable features such as sizeable specific surface area, enhanced electrical charge carrying capacities, optical transparency, exclusive quantum confinement effects that unanimously drive them as well proficient candidates for energy applications, especially as an auxiliary supporting components for imparting desirable flexibility besides electronic and electrochemical reinforcements [32-33]. Although graphenes have been by far the most popular and widely studied 2D systems since the last two decades owing to their exclusive physical and chemical qualities, they do often suffer from serious problems, especially while fabricating diligent electronic gadgets. Graphenes being less hydrophilic and poorly wettable, are hard to be dispersed in suitable solvents to endure classy device manufacturing. Further, the materials' intrinsic conductivity often varies widely with the preparation methodologies. Even the homogeneity in a composition is very hard to accomplish in most cases. Therefore, the challenge for seeking better two-dimensional auxiliary materials

leads to the discovery of MXenes.

MXenes are mostly layered-transition metal carbides, nitrides, carbonitrides, categorized under inorganic-based 2D materials, that are lately gaining huge popularity in this sizzling domain of materials research [33]. Compared to graphene and its derivatives, these materials are more well-composed, mechanically flexible, intrinsically hydrophilic with appreciable electrical conductivity and better solution-processability, showing better adherence to different materials, thus promoting their preferences for 2D-device fabrications [34]. Initially, Gogotsi et al. developed 2D transition metal carbides MXenes via careful etching of 'A' elements from the so-called MAX phases where M denotes early transition metals (such as Ti, Sr, V, Cr, Ta, Nb, Zr, Mo, or Hf.), A signifies main-group elements (mostly IIIA or IVA), and X denotes either carbon or nitrogen as well as both respectively, as indicated in Figure 2(a) [35]. The name with suffix 'ene' has been derived due to their structural resemblance to graphene and are rapidly emerging as one of the frontline materials for various applications in today's technology. Subsequently, wide range of analogous compositions of 2D transition metal carbides, nitrides and carbonitrides have been fabricated within a very short tenure. These compounds bear a general chemical formula of $M_{n+1}X_nT_x$, where M stands for transition metals, X signifies carbon and/ or nitrogen, n = 1, 2, or 3, and T_x denotes surface functional groups (i.e. -O, -OH, -F) respectively, where the X group can be tailored as per utilization necessity [36]. Ti_3C_2, the first "MXene", was obtained by soaking Ti_3AlC_2 [MAX = $(M_{n+1}AX_n)$ phase, where A = group 13-16 elements like Al, Ga, Si, Ge.] powders in hydrofluoric acid solution by different research groups [37-38].
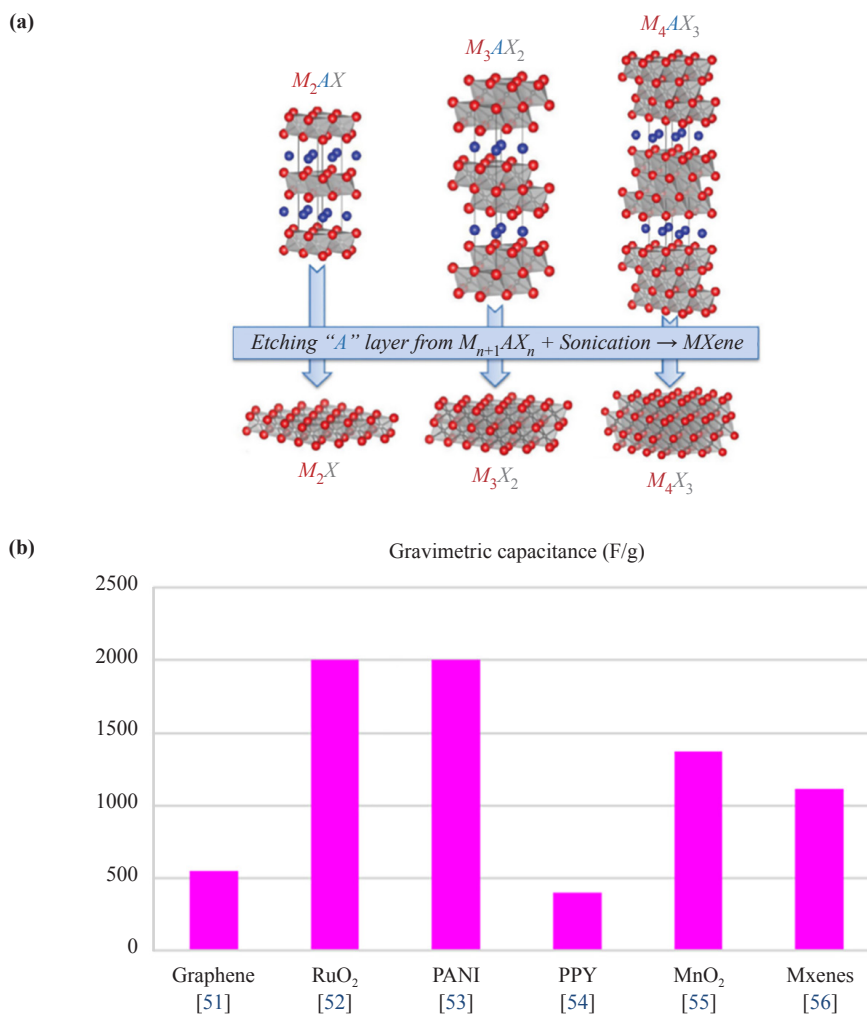
Figure 2. Schematic presentation of various versatile properties of MXenes. Reproduced on permission from ref. [35], copyright © 2013 WILEY-VCH Verlag GmbH & Co. KGaA, Weinheim (a). Comparative chart showing relative theoretical capacitance of some widely popular supercapacitor electrode materials (b) [51-56].

Table 3. Electrochemical performances of MXenes obtained via different methodologies

MXenes	Mode of preparation	Capacitance @ measured voltage sweep rate/ current density, voltage window and electrolyte used	Further details on overall electrochemical performance	Ref
$Ti_3C_2T_x$	Exfoliation of ternary carbides Ti_3AlC_2	Areal capacitance of 579 mFcm^{-2} @ voltage scan rate of 2 mVs^{-1} in 1 M KOH electrolyte, in the voltage window of -0.9 to -0.4 V	Capacitance retention efficacy of 98% after 10000 charging/ discharging cycles	[41]
Nitrogen-doped MXene films	Solvothermal treatment with ex-situ nitrogen doping by urea saturated alcohol or mono-ethanolamine as nitrogen source	Volumetric capacitance of 2836 Fcm^{-3} (gravimetric capacitance of 786 Fg^{-1}) @ voltage scan rate of 5 mVs^{-1} in 3 M H$_2$SO$_4$ solution, in the voltage window of -0.6 to 0.1V	High mechanical flexibility and volumetric energy density of 76 WhL^{-1} displayed by the symmetric electrochemical capacitor	[42]
Nitrogen-doped $Ti_3C_2T_x$ Ink	Melamine formaldehyde templating method	Areal capacitance of 70.1 mFcm^{-2} @ voltage scan rate of 10 mVs^{-1} in polyvinyl alcohol (PVA)/H$_2$SO$_4$ electrolyte, in the voltage range of 0.0-0.6 V	Areal and volumetric energy density of 0.42 mWhcm^{-2} and 0.83 mWhcm^{-3} and 96.2% capacitance retention efficacy after 5000 charging/discharging cycles	[43]
Double-side $Ti_3C_2T_x$ based-micro-supercapacitor	UV laser to cut interdigital patterning technology	Areal capacitance of 52 mFcm^{-2} @ current density of 2 mAcm^{-2} polyvinyl alcohol (PVA)/ LiCl electrolyte, in the voltage range of 0.0-0.6 V	Asymmetric and symmetric device shows voltage window of 0.8 V and 0.6 V respectively	[44]
MXene viscous ink onto 3D printed stamps	Interdigitated stamping strategy	Areal capacitance of 61 mFcm^{-2} @ current density of 25 μAcm^{-2} in in polyvinyl alcohol (PVA)/H$_2$SO$_4$ electrolyte, in the voltage range of 0.0-0.6 V	Areal capacitance of 50 mFcm^{-2} with current density increased by 32 folds.	[45]
3D printed freestanding MXene	Extrusion-based 3D printing	Areal capacitance of 2.1 Fcm^{-2} at 1.7 mAcm^{-2} and gravimetric capacitance of 242.5 Fg^{-1} at 0.2 Ag^{-1} in polyvinyl alcohol (PVA)/H$_2$SO$_4$ electrolyte, in the voltage range of 0.0-0.6 V	Energy density of 0.0244 mWhcm^{-2} and power density of 0.64 mWcm^{-2} @ current density of 4.3 mA cm^{-2} with capacitance retention efficacy of 90% for 10000 cycles	[46]
Li$^+$ intercalated $Ti_3C_2T_x$	$Ti_3C_2T_x$ into LiCl solution followed by vacuum-assisted filtration	Volume capacitance of 892 Fcm^{-3} @ voltage scan rate of 2 mVs^{-1} in 1 M H$_2$SO$_4$ electrolyte, in the voltage range of -0.35 to +0.2 V	No capacitance loss even after 10000 charging/discharging cycles	[47]
$Ti_3C_2T_x$ clay	Etching MAX phase with the HCl + LiF mixed solution	Volumetric capacitance of 900 Fcm^{-3} in H$_2$SO$_4$ electrolyte, in the voltage range of -0.35 to +0.2 V	Recorded high degree of cyclability even after 10000 cycles. The material can be shaped into numerous forms for desired applications	[48]
MXene hydrogel	Gelation method	Gravimetric capacitance of 370 Fg^{-1} @ current density of 5 Ag^{-1} in the voltage range of -1.1 to +0.2 V	Recorded gravimetric capacitance of 65 Fg^{-1} even @ current density of 1000 Ag^{-1}	[49]
$(Mo_{2/3}Y_{1/3})_2CT_x$	Selective etching process	Volumetric capacitance of 1500 Fcm^{-3} in KOH electrolyte, in the voltage range of -0.25 to + 0.3 V and Volumetric capacitance of ≈ 1200 Fcm^{-3} in H$_2$SO$_4$ electrolyte in the voltage range of -0.65 to + 0.3 V	Wide variation in electrochemical properties observed in novel types of atomic laminated phases (coined i-MAX) obtained from different etching protocols of MAX phases, in contrast to other 2D materials reported	[50]

Thus, as the research progressed, simple and productive synthetic schemes attracted the manufacturers to intensively study these materials as they went on finding highly appreciating outcomes, therefore, channelize them into various practical applications of energy storage, sensors, catalysis and several other technological fields [39-40]. Further, MXenes easily form large quantities of fairly pure, aqueous, stable colloidal suspensions that rendered them so popular in easy processable electronics creations. Thus, Table 3 highlights some of the amazing electrochemical performances of different varieties of MXenes used in supercapacitor electrode designing in recent years.

Even though under the current scenario, MXenes fall below in charge storing ability, as indicated in the Figure 2(b), they have been found to be electrochemically as well as mechanically conformable with composition/functionalization and could be assembled into freestanding stretchable electrodes and devices via facile and binder-free fabrication approaches, which place them in healthier positions compared to other recently employed supercapacitor materials such as graphenes, conducting polymers, metal oxides as far as commercialization is concerned. The impressive fact that surface terminal moieties can be autonomously modified has supplementarily promoted appreciable versatility in scheming advanced functional materials with these systems [51-56]. Thus, in a very recent study, Guo et al., had reported areal capacitance as high as 1.399 Fcm^{-2} at a potential scan rate of 1 mVs^{-1} for Ti$_3$C$_2$T$_x$ electrode besides notable cyclic performance even after 17,200 cycles-well succeeding the results obtained for the legendary 3D graphenes (areal capacitance of 1.28 Fcm^{-2} and cycling stability of 86.2% retention after 5000 cycles) [56-57]. Further, single-layered MXenes display tunable energy band gaps with varying chemical composition, unlike graphenes which show zero bandgap property only in pristine single-layered form. Moreover, the absence of dangling bonds in the former permit natural passivation spontaneously. Even their electron mobilities study often records values comparable to or even higher than that of graphenes [58]. Additionally, MXenes own incredibly high Young Modulus values and can withstand large wear resistances with exceptional bending flexibility, which is indeed highly preferable for patterning exquisite wearable electronics [59-61]. Further, ultrathin Ti$_3$C$_2$ based MXenes possess high visible light transmittance ~ 97% to be employed in transparent energy storage electrodes for numerous panel display applications [62].

Recently it was investigated that the electrical properties of MXenes drastically get modified on surface functionalization. The Gibbs free energy of formation calculations indicate the prevalence of O functionalization over -F groups, irrespective of M, X, and n variation, owing to the difference in their formation energies and proposed that the surface functionalization is determined by external conditions and not by the MXene category or layer thickness. Again, the work function of the surface is primarily guided by the dipoles created due to functionalization, thus varies dramatically and linearly, with the nature of the functional group, without too much affecting the density of states at the Fermi level [63]. In another report, it was recommended that the electronic properties of nitrogen functionalized MXenes monolayers can be readily steered by imposing biaxial and uniaxial strains. Notably, the carrier mobility and direct bandgap can be dramatically altered on the introduction of tensile strain that results in structural changes and redistribution of charges brought about by the alterations in bond lengths that result in modified electronic states [64-66]. The terminal functional group strongly affects the net charge storing capability exhibited by the MXene. Of late, computer simulations evidenced better-quality structural, optical and electrical trends through the judicious proposition of surface functionalization [67]. Further, the addition of intercalating units within the layers of MXene sheets largely augments their electrochemical efficacy and electrode durability [68-69]. Lately, the Lukatskaya group investigated the plausible mechanism of high charge storage in functionalized MXenes, Ti$_3$C$_2$T$_x$ in aqueous acid electrolytes probing in-situ X-ray absorption spectroscopy [70]. The results revealed that the spontaneous intercalation of extremely mobile hydronium ions of the acid electrolyte between the Ti$_3$C$_2$T$_x$ layers offered an easy accessibility to the electrochemically active Ti-layers while rapid charge transmission becomes ensured by the high electron density C-layers. The terminal oxygen and other highly electronegative groups on the Ti$_3$C$_2$T$_x$ surface undergo bonding interactions with hydronium ions in H$_2$SO$_4$ upon discharging, while getting detached upon charging, reinforcing continuous changes of titanium oxidation state during the charging/discharging cycling processes [71-72].

Nonetheless, MXenes like graphenes as well as several other nanosystems undergo spontaneous self-aggregation owing to strong cohesive interactions controlled by inter-layer van der Waals attractions and hydrogen bonding that ultimately results in considerable loss in their substantial surface area, electroactive sites availability and inhibit rapid ions exchange process resulting in impaired electrochemical performances. To combat this problem, various strategies have been implemented to improvise the morphology of the MXene electrodes so as to improve their surface accessibility, conductivity as well as ion transfer characteristics. These embrace construction of microporous Ti$_3$C$_2$T$_X$ hydrogel films besides engineering appropriate composite electrodes. Some of these strategies have been considerably effective in upgrading the ion transport and electrode performances, but cut down the electroactive material concentration resulting in reduced volumetric capacitance, energy density, particularly thick-film electrodes. Thus, appropriate composites fabrication with well-suited tailored architectural patterns has been globally suggested to optimize not only the electrochemical but also its structural robustness for a wider domain of functional applications [73-74].

2. MXenes/PANI nanocomposites as smart electrode materials for supercapacitors

2.1 *MXenes/PANI binary composites as supercapacitor electrode materials*

Composite formation through surface modification and precise morphological nanoengineering procedures often promotes proper synergistic combinations of the electric double-layer capacitance and the pseudocapacitive contributions of both the components that cumulatively boost the material's electrochemical energy storage efficacy [75]. Thus, the MXenes and the PANI, two well-capable pseudocapacitive materials have been proposed to be appropriately blended in the right proportions to synergistically upgrade the overall electrochemical performances. Accordingly, various synthetic propositions have come up for developing MXenes/PANI binary nanocomposites for supercapacitor applications as illustrated in Figure 3.
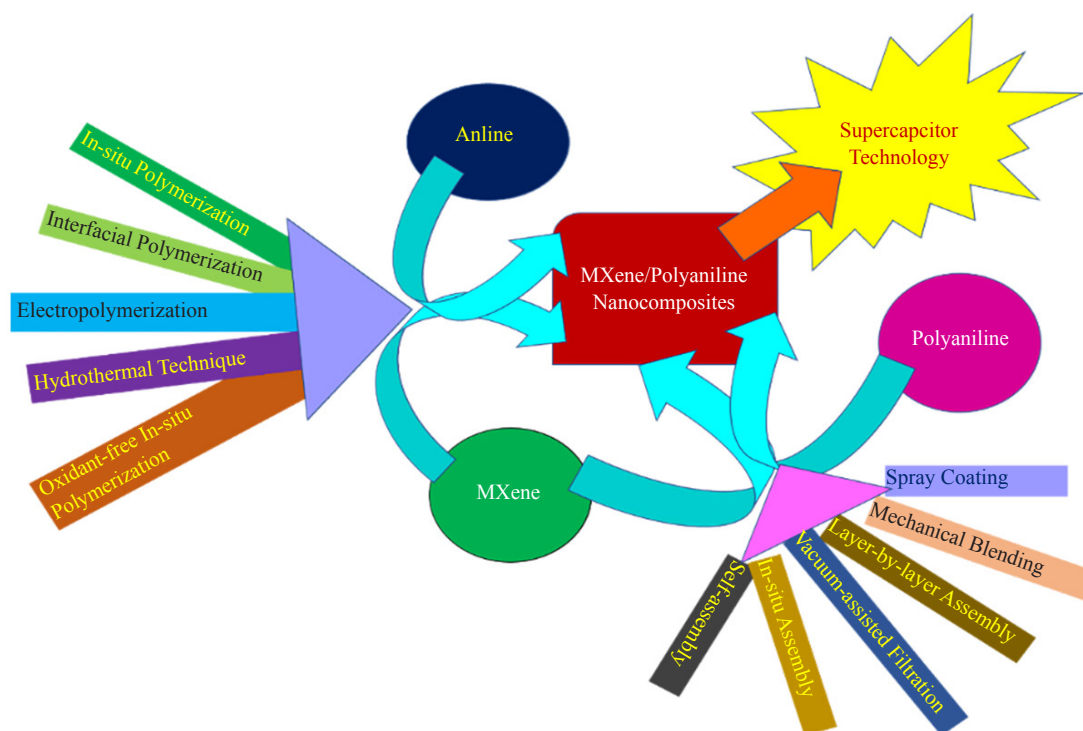
Figure 3. Various synthetic techniques developed for fabricating MXene/PANI nanocomposites for supercapacitor applications

Some of these MXenes/PANI nanocomposites, depending on their synthesis methodologies and nature of electrolytes employed for electrochemical investigations have shown great variations in their relative capacitive performances as having been outlined in Table 4. The benefits obtained on nanocomposite formation relative to their individual components have also been focused to highlight the essence of hybridization of the constituents in suitable proportions to reinforce their overall responses.

Table 4. Electrochemical performance of some MXene/PANI binary nanocomposites obtained via different fabrication procedures

Composite electrode	Fabrication methods	Electro-lytes	Voltage window	Capacitance	Cyclic performance	Cell type and performances	Benefits of nanocomposite formation	Ref
Ti₃C₂/PANI-nanotubes	Exfoliated ultrathin Ti₃C₂ nanosheets subjected to one-pot in-situ polymerization for their surface decoration by PANI nanotubes	1 M H₂SO₄	-0.2 V to +0.8 V	300.8 Fg⁻¹ (@ Current density of 0.1 Ag⁻¹)	94.7% after 5000 cycles (@ 1 Ag⁻¹)	Symmetric cell, cell voltage of 1.8 V, Max. specific energy of 25.6 Whkg⁻¹ and Max. specific power of 1610.8 Wkg⁻¹ @13.2 Whkg⁻¹, and cycling stability of 81.1% capacitance retention after 4000 cycles	The hierarchical micro-structured nanocomposite displayed improved electrochemical features such as the longest discharge time and higher specific capacitance compared to pristine PANI nanotubes and Ti₃C₂ MXene under similar experimental conditions	[76]
Ti₃C₂Tₓ/PANI	Oxidant-free in-situ polymerization of PANI on the MXene sheets surfaces	3 M H₂SO₄	-0.7 to +0.2 V	1163 Fcm⁻³ (@ potential sweep rate of 2 mVs⁻¹)	98.3% after 10,000 cycles	Symmetric cell, cell voltage of 1.0 V, Energy density of 79.8 WhL⁻¹ @ power density of 575 WL⁻¹	The thick and freestanding hybrid nanocomposite electrode displayed higher volumetric capacitances even for thick electrodes compared to pristine MXene electrodes	[77]
N-Ti₃C₂/PANI	Two-stage of electrochemical reactions via chemical grafting	0.5 M H₂SO₄	0-0.5 V	228 mFcm⁻² (@ potential sweep rate of 5 mVs⁻¹)	85% after 1000 cycles @ 1 mAcm⁻²	-	The capacitance of N-Ti₃C₂/PANI nanocomposite electrode is enhanced by 32 times compared to that of pristine Ti₃C₂ electrode	[78]
PANI/Ti₃C₂Tₓ	Composite ink coating technique	1 M H₂SO₄	-0.2 to +0.8 V	560 Fg⁻¹ @ potential sweep rate of 5 mVs⁻¹	71.2% after 5000 cycles @ 30 Ag⁻¹	Asymmetric cell PANI/Ti₃C₂Tₓ/Ti₃C₂Tₓ; cell voltage of 1.4 V; Energy density of 65.6 WhL⁻¹ @ power density of 1687.3 WL⁻¹ and cycling stability of 87.5% capacitance retention after 5000 cycles	The self-supporting PANI/MXene flexible film electrode showed improved capacitive response compared to pristine PANI electrode	[79]
Ti₃C₂Tₓ/PANI	Direct assembly procedure	1 M H₂SO₄	0.0-0.8 V	556.2 Fg⁻¹ (@ current density of 0.5 Ag⁻¹)	91.6% after 5000 cycles @ 5 Ag⁻¹	-	The MXene/PANI composite electrode recorded improved electrical conductivity, specific capacitance, rate capability and capacitance retention efficacy with appreciable cycling stability compared to its constituent electrodes	[80]
Ti₃C₂Tₓ/PANI	Hydrothermal technique	7 M KOH	0.0-1.0 V	592 Fg⁻¹ @ current density of 0.5 Ag⁻¹	95.3% after 10000 cycles @ 5 Ag⁻¹	Asymmetric cell MXene/PANI//AC cell voltage of 1.2 V; Specific Energy of 22.67 Whkg⁻¹ @ power density of 0.217 Wkg⁻¹	The MXene/PANI//AC cell recorded higher cell capacitance and coulombic efficacy than the MXene//AC asymmetric cell	[81]
PANI-Ti₃C₂	In-situ polymerization technique	1 M Na₂SO₄	-0.8 V to -0.2 V	164 Fg⁻¹ @ potential sweep rate of 2 mVs⁻¹	96% after 3000 cycles @ 3 Ag⁻¹	-	The gravimetric capacitance of PANI-Ti₃C₂ electrode is 1.26 times larger than that of pristine Ti₃C₂ (131 Fg⁻¹ @ potential sweep rate of 2 mVs⁻¹)	[82]
Ti₃C₂Tₓ/PANI-nanofibers	Self-assembly technique	3 M H₂SO₄	-0.70 V to +0.25 V	959.1 mFcm⁻² (645.7 Fg⁻¹) @ potential sweep rate of 10 mVs⁻¹	98% after 5000 cycles @ potential sweep rate of 10 mVs⁻¹	-	The flexible freestanding Ti₃C₂Tₓ/PANI-nanofibers composite electrode displayed higher conductivity (1373.3 Scm⁻¹), gravimetric capacitance, improved structural and cycling stability than that of pristine Ti₃C₂Tₓ electrode (750.0 mFcm⁻² and 84.6% after 5000 cycles)	[83]
PANI@microporous-Ti₃C₂Tₓ	Casting homogenous polyaniline layer on 3D porous MXenes	3 M H₂SO₄	0.0-0.6 V	510 Fg⁻¹ (1632 Fcm⁻³) @ potential sweep rate of 10 mVs⁻¹	-	Asymmetric cell, M-Ti₃C₂Tₓ//PANI@ M-Ti₃C₂Tₓ (cell voltage of 1.2 V, Energy density of 50.6 WhL⁻¹ @ power density of 127 kWL⁻¹	The nanocomposite formation caused Fermi level shift compared to pure MXene that modified the electronic structure and developed higher resistance toward electron loss, resulting in greater ability to endure anodic potential and display higher positive operating potentials	[84]

Comprehensive research narrates that there exist two general modes of MXenes/PANI nanocomposites preparation approaches. The first type of fabrication strategy involves mixing and adsorption of aniline monomers on the well-delaminated MXenes sheets followed by various polymerization procedures, of which the most popular ones are the in-situ polymerization, interfacial polymerization, electropolymerization, oxidant-free in-situ polymerization, hydrothermal assisted polymerization reactions, etc. Each of these synthesis processes has their own uniqueness. For instance, in-situ polymerization mediated synthesis ensured uniform dispersion of polymer nanophase over MXene layers for better interfacial charge transfer contacts. Again, the Oxidant-free polymerization mediated approach has been advantageous as it successfully avoided the unwanted use of non-green chemical reagents as well as inevitable surface contaminations in a controllable synthesis condition. This strategy was applied to modify the surface of MXene sheets by PANI in order to design pseudocapacitive electrodes with large accessible architecture and improved electrochemical efficacy even for very thick constructions [77]. Further, electropolymerization aided preparation techniques have been applied to promote the well-controlled formation of layered PANI depositions on the MXene sheets [85].

The other integrating strategy of constructing MXene/PANI nanocomposites involves the preparation of individual PANI and MXenes components separately and assembling them through suitable methodologies to design the desired electrode material. One such approach involves a layer-by-layer assembly technique that has been employed to design PANI nanofiber/MXene composite electrodes for detailed study of charge storage mechanism prevailing therein the electrodes to be discussed in a while. The layer-by-layer assembly technique is a facile synthesis procedure that employs electrostatic interactions between positively charged PANI and the hydrophilic and negatively charged MXene. Thus, Yin et al. fabricated multifunctional MXene/PANI composite textile by the layer-by-layer assembling of PANI nanowires and MXene nanosheets onto a carbon fiber fabric substrate for developing flexible and wearable electronics [86]. Likewise, the Wang group developed a solvent-mediated self-assembly technique followed by a redispersion approach to obtain PANI/MXene inks that were further utilized in designing PANI/MXene composite films vide evaporation-induced assembly procedure. The resultant compact interlayered heterojunction-based MXene/PANI electrodes demonstrated ultrahigh volumetric capacitance (1167 Fcm^{-3}), ultrafast electron and ionic activities, besides preventing restacking of MXene sheets. Thus, here the hierarchical morphology and the synergistic understanding between PANI and $Ti_3C_2T_x$ are responsible for the superior capacitive performance of this nanocomposite as indicated in the data provided in Table 4 [79]. Analogously, in another work, sandwiched porous structure of the composite was obtained via self-assembly of PANI nanofibers placed as conductive interlayer spacers in-between the MXene layers. The electrostatic and hydrogen bonding interactions prevailing among the positively charged PANI nanofibers and negatively charged MXene nanosheets brought about excellent chemistry in the resultant nanohybrid. Accordingly, the flexible binder-free nanocomposite electrode displayed high conductivity (1373.3 $S.cm^{-1}$) much improved electrochemical performance compared to that of the pristine $Ti_3C_2T_x$ electrode [83].

While investigating the prospects of effective strengthening of the bonding interactions between the constituents in the resultant nanocomposite, Ren et.al, indicated that the amino groups of PANI within PANI/Ti_3C_2 nanocomposite significantly improved the electrical conductivity as well as surface wettability, thereby upgrading the overall electrochemical performance owing to the cooperativity between the components [82]. In an alternative preparation strategy, chemical bonding between N-functionalized Ti_3C_2 and PANI chains electrochemically deposited on FTO-glass substrate established organ-like structured supercapacitor electrode successfully. The unique morphology was introduced due to the presence of robust chemical bonds between the components that also synergistically reduced the charge transfer barrier and afforded ultrafast charge transfer kinetics as well as enhanced the electrochemical stability by avoiding easy coalescence of MXene sheets. Moreover, the N-sites of MXene were found to serve as active centers to effectively interact with the aniline monomers and promote directional PANI growth over the surfaces of the Ti_3C_2 layers that result in elevating the capacitance of the optimized composite by nearly 32 times to that of pristine MXene [78]. Additionally, it has been evidenced that the nature of surface functional moieties on MXenes facilitate the easy and controlled nucleation of the aniline polymerization process as well [80]. In the very recent time, MXene layers surface-anchored with chain-like PANI wrapped by PANI nanofibers were obtained by simple, cost-effective and well-controlled hydrothermal technique that demonstrated a high capacitance rate capacity of 84.72% on increasing the current densities from 0.5 to 20 Ag^{-1} along with capacitance retaining the efficacy of 95.15% even on surpassing 10000 charging/discharging cycles [81]. The existence of durable chemical interactions between PANI with MXenes sheets placed in-between the layers has been frequently confirmed by several characterization techniques including FTIR,

RAMAN, XPS, powder-XRD, besides morphological imaging obtained from electron micrograph studies. Lately, titanium carbide ($Ti_3C_2T_X$) MXene has been employed as a conducting binder for PANI electrodes that considerably improved the capacitance retention efficacy to 96 % even after completing 10000 cycles @ high potential scan rate of 50 mVs^{-1} as well as high-rate capability, on just applying 15 wt% of $Ti_3C_2T_x$ MXene binder. The authors justified that, unlike commonly used insulating polymer binders that itself introduce a charge barrier within the PANI electrodes, MXene is superior as they are metallic conducting in nature. Besides, the easily processable MXene also contributes to intrinsic redox capacitance that cumulatively upgrades the overall electrochemical performance of the conducting polymer electrodes besides offering high mechanical strength wing to the presence of polar surface functional groups on MXene that strongly bind the polymer chains to augment the cyclic activity of the electrodes [87]. Further, Chen et al. employed DL-Tartaric acid (DLTA) to initially self-assemble on the MXene surface followed by aniline polymerization induced by the electronegative oxygen moieties on the DLTA. The organic acid also served as a suitable doping agent for PANI to promote better electron transport in the resultant composite besides announcing large spatial distribution flexibility owing to the presence of copious oxygen-containing functional groups like -OH, -COOH that accomplish supramolecular self-assembling with MXenes via multiple hydrogen bond connections in addition to chiral interactions. [88]. The comparative characterization of the constituent electrodes and the MXene-DLTA/PANI (TDPs) nanocomposite electrode with optimal composition clearly delineates the existence of synergistic influence on the electrochemical signatures of the latter produced by a collective cooperative effect, well superior to the summation of their individual contributions, as indicated in the profiles given in the Figure 4 (a-d) [88].

Similar bonding illustrations have been observed in the macromolecularly interconnected 3D graphene/ nanostructured conductive polymer hydrogels with high mechanical flexibility, where the authors have inferred that such unique self-assembled features have originated from hydrogen bonding interactions originating from the N-H group of PANI molecules and terminating oxygen on the surface of MXenes nanosheets [89]. Such tie-up interactions facilitate the growth of specific PANI nanostructures with porous architecture on MXene layers to boost the overall conductivity of the composite as well as amplify the pseudocapacitive output [90]. Lately, amphiphilic cetyltrimethylammonium bromide (CTAB) surfactant was employed to initiate self-assembly among the components to uplift the performance of $Ti_3C_2T_x$/PANI nanocomposite. Electrochemical investigations confirmed that the co-intercalation of CTAB introduces higher electrochemical activity as well as reversibility. The designed nanocomposite achieved about 1.43 times greater gravimetric capacitance than that of surfactant-free-$Ti_3C_2T_x$/PANI composite besides enduring high-rate capability [91]. In another investigation, negatively charged hydroxyl-terminated MXene ($Ti_3C_2T_x$) interacted with positively charged emeraldine salt-based PANI nanosheets dispersed in the N-methyl pyrrolidone solvent to favor homogeneous PANI coating on the MXene surface, thereby promoting the formation of three-dimensional morphological architecture with a sizeable electrolyte-accessible surface in the resultant PANI/hydroxyl-terminated $Ti_3C_2T_x$ composites. The so-obtained composite electrode recorded a notable gravimetric capacitance of 464 Fg^{-1} @ 1 Ag^{-1} current density, which is being much superior to that recorded for the emeraldine-based PANI electrode (307 Fg^{-1}) and PANI/pristine-$Ti_3C_2T_x$ composite electrodes (348 Fg^{-1}) respectively, as well as demonstrating larger cyclic stability at high current density, hence justifying the above realization [92].

Drive for a detailed understanding of charge storage mechanism and the part played by the components therein, lead to some interesting results in the recent past [74]. Vahid and his coworkers reported that the high gravimetric capacitance and outstanding rate capability of $Ti_3C_2T_x$/PANI films were attributed to the widened interlayer spacing of MXene sheets in the composite electrodes that facilitated faster ion transport within the electrode as well as upgraded ion accessibility to the redox-active sites on the MXene surface. It is important to note the experimental voltage window understudy is crucial to explain the mechanistic charge storage process in these nanocomposites using the suitable electrolytes. As in the present case, the authors chose the potential window to study the electroactivity of the hybrid electrode using acidic aqueous electrolytes (-0.7 V to + 0.2 V vs. Ag/AgCl) where PANI is found to be electrochemically idle and MXene exclusively contributes to the overall pseudocapacitive response. Therefore, in this case, PANI mainly played as a conductive spacer to augment the ionic and electronic conductivity in the fabricated electrodes, as confirmed by the electrochemical impedance studies. It is worth perceiving that PANI serves as a much better conductive spacer compared to other nano-carbons, such as CNT, graphene, etc. as the former can be readily wrapped on the MXene sheets precisely by monitoring the $Ti_3C_2T_x$ to aniline mole ratio during the synthesis process and thus restricting auto-agglomeration and restacking of MXene sheets and thereby promoting higher effective electroactive surface utilization

efficacy [77].
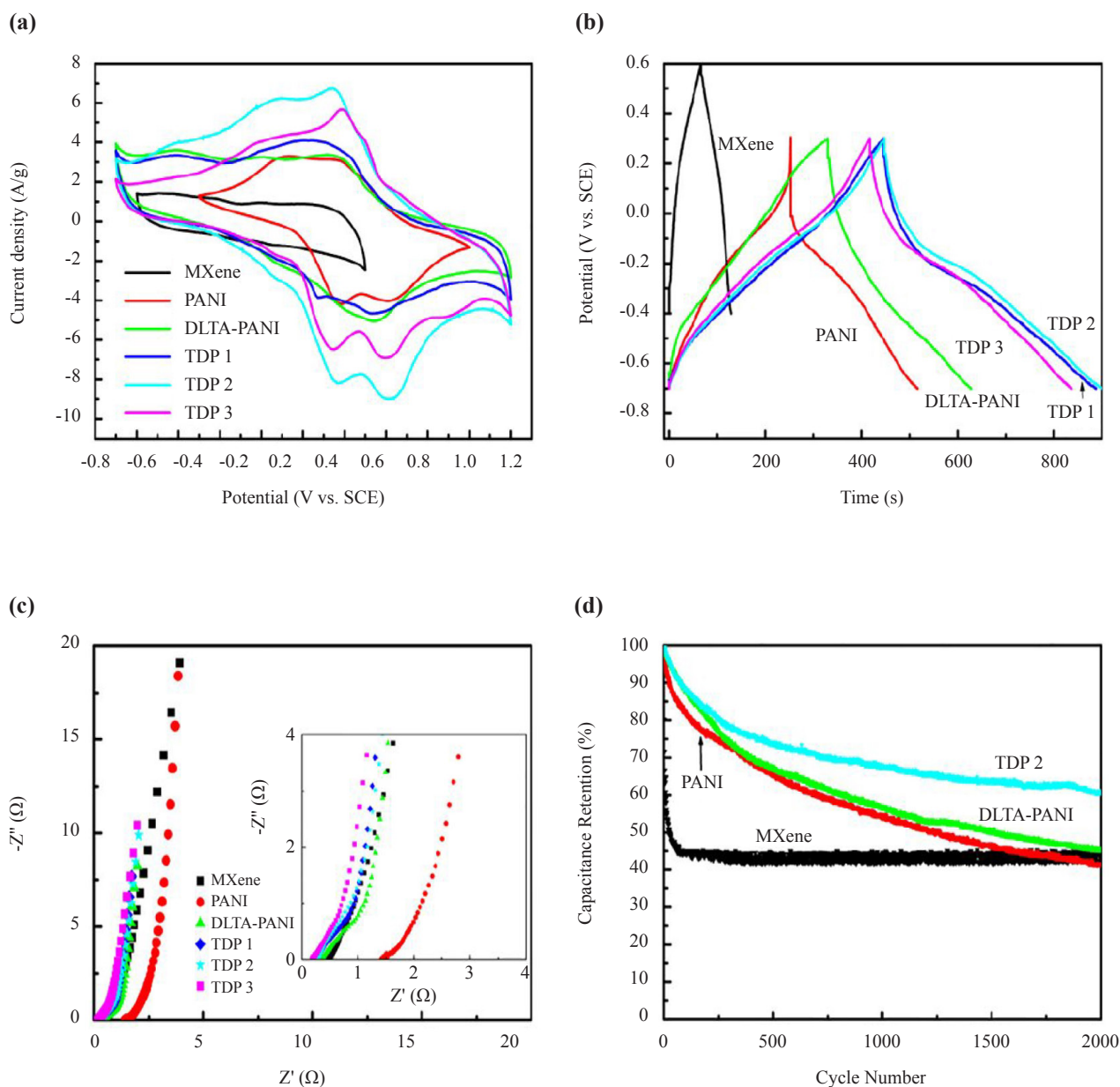
Figure 4. Comparative cyclic voltammograms of pristine-MXene, pure-PANI, DLTA-PANI and MXene-DLTA/PANI (TDPs) sample electrodes at a voltage sweep rate of 10 mVs⁻¹ (a), Comparative galvanostatic charging/discharging profiles of pristine-MXene, pure-PANI, DLTA-PANI and MXene-DLTA/PANI (TDPs) electrodes at a current density of 1 Ag⁻¹ (b), Nyquist plots of pristine-MXene, pure-PANI, DLTA-PANI and MXene-DLTA/PANI (TDPs) samples (c) and Comparative capacitance retention efficacy of pristine-MXene, pure-PANI, DLTA-PANI and optimized-MXene-DLTA/PANI (TDP2) sample electrode at a constant current density of 4 Ag⁻¹ for 2000 cycles (d). Reproduced on permission form ref. [88], copyright 2020, ACS publications

As far as energy storage device fabrication is concerned, provision for designing symmetric supercapacitors requires the employment of the same electroactive material as both anode and cathode with appreciable chemical stability in the working electrolytes. Accordingly, a MXene/PANI nanocomposite prepared by single-pot reaction involving delamination in combination with simple organic acid assisted in-situ polymerization technique was set for

symmetrical supercapacitor device in 1 M H_2SO_4 electrolyte that illuminated up a 1.8 V LED bulb. Here, the in-situ polymerization promoted PANI chains to get inserted and anchored on the MXene surface via intimate non-covalent interactions that resulted in their self-assembling to form doped PANI hollow nanotubular morphology decorated on the MXene surface. Such tubular structure also favored faster charge transport besides preventing the MXene sheets from restacking and self-collapsing. The device exhibited utmost specific energy of 25.6 Whkg^{-1} (@ specific power of 153.2 Wkg^{-1}) along with appreciable cyclic stability (81.1% capacitance retention efficiency even after 4000 charging/discharging cycles). The authors claimed that the open and interlocking hierarchical morphology initiated better ion accessibility, electronic mobility that boosted the electrochemical properties cumulatively [76]. However, the urge for higher capacitance, operating voltage window to endorse high device energy and power densities drives for cell assembling in asymmetric configuration with suitable cathode and anode materials with supportive electrolytes. The suitable choice of electrolytes complementing the electrode materials to assure a wide operating voltage domain is a worthful task, especially with cost-effective aqueous electrolytes that work under a narrow operating voltage range. Thus, the Li group proposed hierarchical architecture-based PANI-MXene nanocomposite cathode having a 3D porous MXene $Ti_3C_2T_x$ network coated with a uniform PANI layer for devising an aqueous acid electrolyte based asymmetric supercapacitor cell. The resultant electrode recorded a high volumetric capacitance of 1632 Fcm^{-3} with excellent rate capability, displaying capacitance as high as 827 Fcm^{-3} even at high voltage sweep rates of 5000 mVs^{-1}. Further, this remarkable cathode material was coupled with pure-MXene anode yielding a large volume energy density of 50.6 WhL^{-1} @ ultrahigh volume power density of 127 kWL^{-1}, acquiring cell voltage as high as 1.4 V, which is decent for aqueous-based energy storage systems [84].

Unlike pristine MXenes that show capacitive response in the negative potential range, the integrated PANI/MXene heterostructures display good capacitive behavior in the positive voltage zone, enabling stable operation of MXene at positive potentials owing to the distended work function after composite formation with PANI thus favoring the combinations of MXenes and PANI/MXene composite heterostructures in designing asymmetric supercapacitor cells with wider operational voltage window. Hence, the derived all-pseudocapacitive compact film cell delivered an incredible wide operating voltage of 1.4 V using 1 M H_2SO_4 aqueous electrolyte, securing a large volume energy density of 65.6 WhL^{-1} @ power density of 1687.3 WL^{-1} signifying the high degree of effectiveness of the assembled cell configuration [93]. Very recently, the PANI/$Ti_3C_2T_x$ nanohybrid electrode was obtained by adopting a simple and economic technique via self-assembling of PANI nanofibers and $Ti_3C_2T_x$ nanosheets. It was employed to set up an asymmetric cell by combining PANI/$Ti_3C_2T_x$ nanohybrid as the positive electrode and carrot-derived porous carbon as negative electrode respectively that demonstrated utmost energy density of 50.8 Whkg^{-1} @ 0.9 kWkg^{-1} and an output voltage of 1.8 V in the aqueous electrolyte which was further upgraded to 67.2 Whkg^{-1} @ 1.5 kWkg^{-1} with extended voltage window of 3 V in organic electrolytes correspondingly [94].

Lately, lower resistance-based highly pseudocapacitive V_2C MXene instead of widely popular Ti_3C_2 one was deployed for better designing of integrated sensing devices. Thus, PANI/V_2C nanocomposites with the outstanding capacitive performance of 337.5 Fg^{-1} at 1 Ag^{-1} current density, was employed to fabricate the button-type miniatured asymmetric supercapacitor using PANI/MXene anode and active carbon as cathode, demonstrated substantial specific energy of 11.25 Whkg^{-1} and the specific power of 415.38 Wkg^{-1} respectively in addition to high electrochemical stability, retaining 97.6% of initial capacitance even after completing 10,000 charging/discharging cycles [95]. As far as the fabrication of portable and miniatured thin-film energy storage devices are concerned; they must accomplish a high energy density for designing high-tech electronic devices. Such construction requires the electrode material to be readily deposited with controllable thickness to deliver appreciable energy and power. Thus, Yun et al. showed that depending on the composition and number of the component layers formed in the prepared nanocomposite electrode, obtained via layer-by-layer technique, the contributions of Faradaic and non-Faradaic capacitive processes were found to get varied accordingly with voltage sweep rates, as illustrated in Figure 5(a-b). Thus, this simple "layer-by-layer assembling" fabrication technique warrants controlled film layer thickness for each component in the nanocomposite although it is often found to be sluggish and laborious, leading to composite films of moderate stability [96].

(a) <Lower scan rate region_1-10 mV s^{-1}>

(b) <Higher scan rate region_10-100 mV s^{-1}>
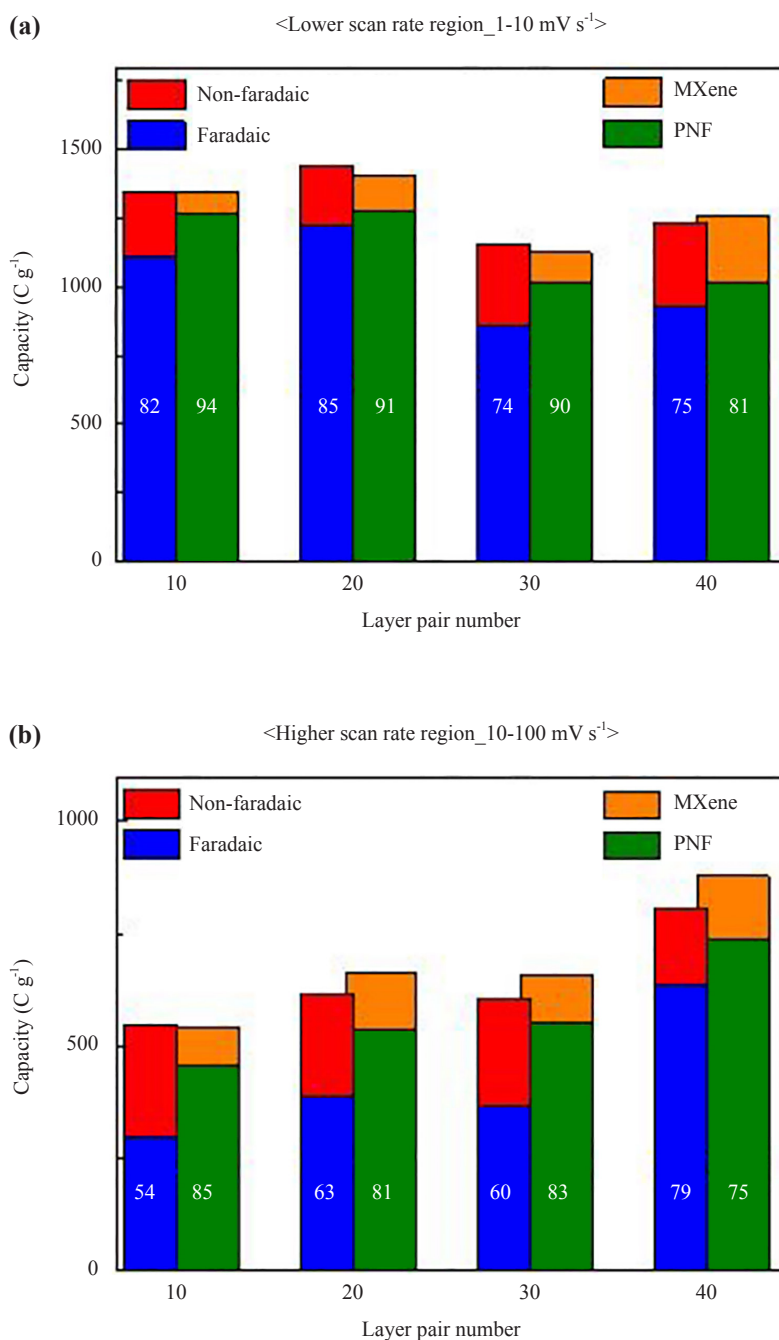
Figure 5. Relative contributions from non-Faradaic (red) and Faradaic (blue) processes bar from MXenes (orange) and PNFs (olive) as a function of the number of layer pair numbers (a) at the slower potential scan rate regime (1-10 mVs^{-1}) and (b) at the higher potential scan rate regime (10-100 mVs^{-1}). Reproduced on permission from ref. [96] ACS publications.

2.2 MXenes/PANI ternary composites as supercapacitor electrode materials

Thus, it is evident that the PANI/MXene binary nanocomposites have been extensively explored due to their promising electrochemical and structural features, particularly in terms of improved cooperative pseudocapacitance behavior, electrochemical stability, mechanical tenacity for advanced energy storage implementations. Nonetheless, they do often lack efficient smooth boundaries and inter-intra-grain contacts to minimize interfacial resistances that drastically deteriorate their charge transport kinetics and result in inferior energy values and so highly urges further

necessary improvements. Therefore, strategies to intimately blend three components in the appropriate extents to assure synergistic contributions through mutual synchronization of their benefits and setting aside individual shortcomings to accomplish utmost device efficacy [97]. Consequently, various ternary nanocomposites with PANI and MXenes as common components have been fabricated, as indicated in Table 5, showing diverse architectural and electronic features with fruitful outcomes not only in accomplishing larger capacitive performances due to the increased degree of redox-active sites, preferential morphology for faster electrons/ions transfer kinetics, uncomplicated interfacial chemistries but also in enhancing mechanical features for manufacturing smarter electronic accessories [98-102]. Thus, MXene-CNT/PANI ternary nanocomposite electrode was constructed with optimized composition by inserting PANI-coated CNTs in-between the MXene layers that synergistically supported improved electron and ion transfer processes for improved overall capacitive response, as illustrated in Figure 6(a) [98]. Here, the MXene nanosheets and PANI collectively contributed to the electrode pseudocapacitance by providing a larger number of electroactive sites for smooth occurrence of Faradaic capacitive charge storage processes. Besides, the interconnected network structure promoted ultrafast electron transmission channels supported by high conducting CNTs. Again, the tubular-like morphology greatly improved the ion accessibility besides holding back the self-assembling tendency of MXene nanosheets. Further, the architecture very well assisted in withstanding the abrupt volume changes in PANI while undergoing a large number of charging/discharging cycles thereby upgrading the cycle stability of the resultant ternary nanocomposite electrode. Accordingly, the best composition electrode accomplished enhanced capacitance as good as 429.4 Fg^{-1} @ current density of 1 Ag^{-1}, with much decent and stable cyclic performance, retaining 93% of original capacitance even after 10,000 cycles, the results declaring far improved capabilities compared to its individual component electrodes [98]. To impose good extent of cooperatively among the unique properties of graphene, MXene and PANI, Wang and his co-researchers effectively equipped a two-dimensional layered graphene-decorated $Ti_3C_2T_x$/PANI nanocomposite, that accomplished superior capacitive performance, large voltage window, and decent electrochemical stability owing to the synergistic influence among the three constituents while working as the cathode materials in asymmetric supercapacitor cell [99]. Likewise, Fu et al. reported a mechanically flexible graphene-encapsulated accordion-type MXene-Ti_2CT_x@PANI (GMP) composite-based supercapacitor electrode in a systematic and steady configuration that exhibited enhanced electrochemical features. The resultant ternary nanocomposite electrode recorded high gravimetric and outstanding volumetric capacitances of 635 Fg^{-1} and 1143 Fcm^{-3} respectively @ 1 Ag^{-1} current density besides displaying improved capacitance retentive competence of 97.54% even on completing 10,000 charge/discharge cycles, credited to the synergistic impact subsidized by the intercalated graphene and conductive PANI in-between the MXenes layers. Herein, besides the multi-benefits of PANI/MXene nanocomposite, the inclusion of conducting graphene sheets provides additional stability towards enduring volume fluctuations during the charging/discharging processes, leading to improved capacitance and notable cycle stability. The obtained energy and power densities of the asymmetric cell designed using the ternary nanocomposite and graphene (GMP//graphene) as reflected in the Ragone plot in the Figure 6(b), which visibly illustrates its impressive electrochemical performances relative to many other composite electrodes found in the literature, justifying its higher potentiality in practical energy storage devices [100].

The rapid progression of light density, portable and comfort-fabric-based wearable and wrappable electronics mandates the deployment of highly flexible, featherlight, miniaturized and extremely competent energy-storing components with auto-powering benefits. This ground-breaking idea has been further endorsed to fabricate microscale, self-powering implanted bioelectronics, where the functional supercapacitor materials should score good biocompatibility, wet-adhesiveness, stretchability along with high electrochemical performances. Consequently, PANI@rGO/Mxenes ternary nanocomposite gel electrodes possessing exceptional electrochemical efficacy, tied with in-situ cross-linked hydrogel electrolyte as well as encapsulating case was used to design all-hydrogel micro-supercapacitors. The resultant energy storage system was found to be air-light, miniatured and portable, besides being flexible, stretchable, and wet-adhesive in character. The designing strategy not only facilitated robust interfacial interactions among gel electrodes and gel electrolytes for securing large areal capacitance and energy density but also benefited the development of multifunctional bio-integrative electronics on wet tissues and vital body organ units with appreciable in-vitro and in-vivo biocompatibility [101].
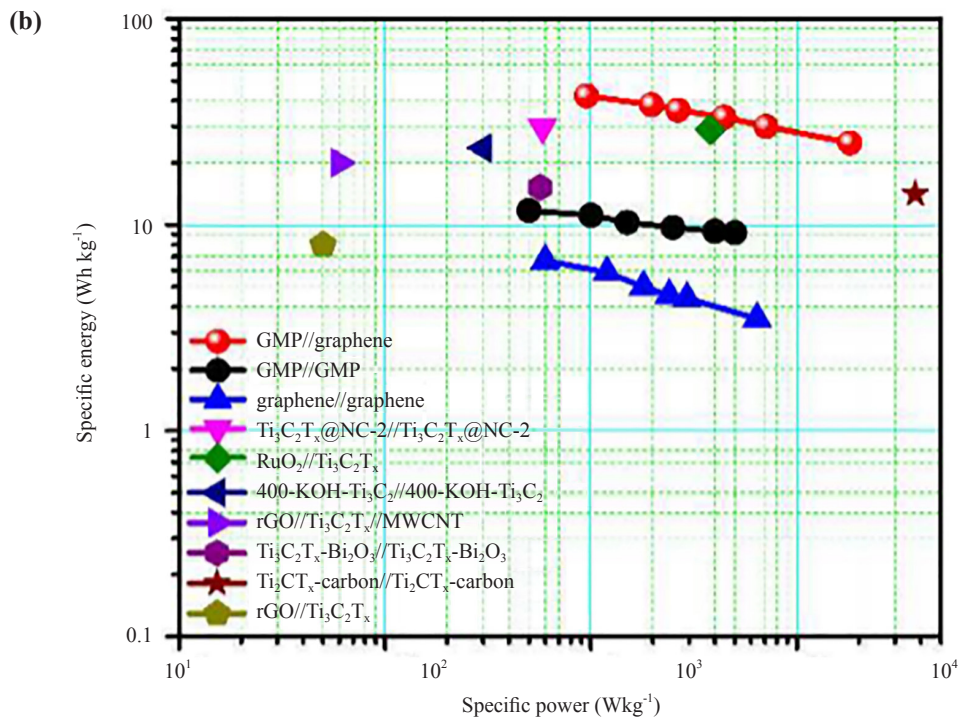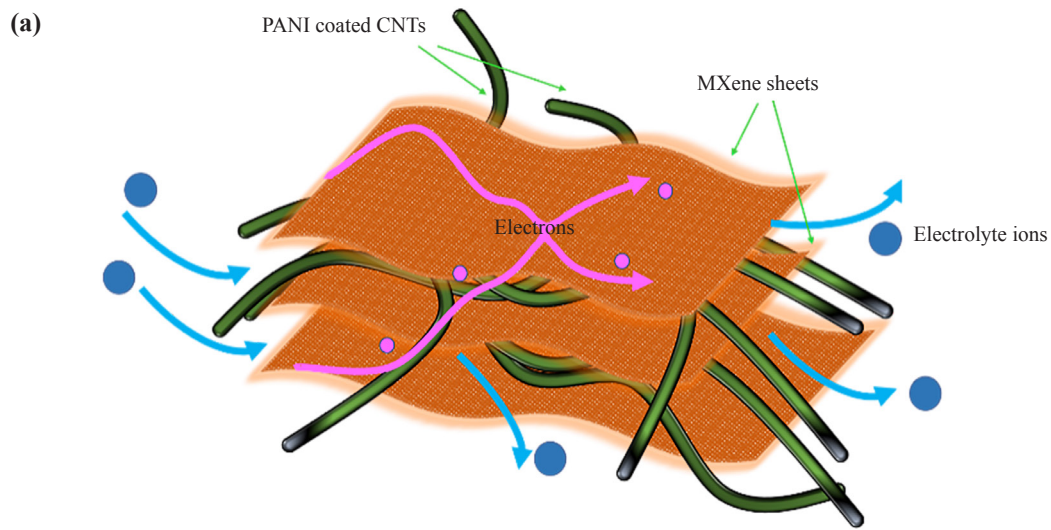
Figure 6. Schematic presentation of the operating charge transport and storage mechanism in MXene-CNT/PANI ternary nanocomposite (a). Ragone plot highlighting the improved electrochemical performances of the Graphene-Encapsulated MXene $Ti_2CT_x@PANI$ (GMP) composite based asymmetric supercapacitor (GMP//graphene) relative to various other composites already reported in the literature (b). Reproduced on permission from ref. [100], copyright 2018, ACS publications

Similarly, for better surface area accessibility and better ion insertion/extraction pathways, hierarchical PANI@ $TiO_2/Ti_3C_2T_x$ ternary composite was fabricated by introducing PANI nanoflakes and TiO_2 nanoparticles in between MXene layers for improved pseudocapacitance and increased surface-active densities. In the nanocomposite, the improvement in electrical conductivity, effective active materials utilization of pseudocapacitive PANI and TiO_2 as well as mechanical stability were ensured by the two-dimensional $Ti_3C_2T_x$ in the ternary composite. The resultant nanosystem electrode exhibited improved gravitational capacitance of 188.3 Fg^{-1} at a potential sweep rate of 10 mVs^{-1},

twice greater than that of binary $TiO_2/Ti_3C_2T_x$ electrode in KOH electrolyte. Furthermore, it also attained remarkable cyclic performance, with capacitance retaining the efficacy of 94% even after 8000 charging/discharging cycles @ a current density of 1 Ag^{-1} [102]. Analogously, in another report, ternary MXene/MnO_2/polyaniline nanostructures were efficaciously planned via facile, scalable, and reproducible bi-step chemical technique involving hydrothermal reaction for growing interlaced layered MnO_2 in-between the MXenes sheets and surfaces followed by chemical oxidative polymerization reaction of aniline at low temperatures. The resultant accordion-type morphology offered highways for fast electron conduction while highly pseudocapacitive MnO_2 nanosheets inhibited the MXene layer restacking and accelerated ion diffusion and transfer processes. The outer PANI layer coating further improved the overall electrochemical response of the composite, registering capacitance of 216 Fg^{-1} at a current density of 1 Ag^{-1} along with improved cyclic stability of 74% after undergoing 5000 cycles using the two-electrode testing system [103].

Table 5. Electrochemical performance of some MXene/PANI ternary nanocomposites obtained via different fabrication procedures

Composite electrode	Fabrication methods	Electro-lytes	Voltage window	Capacitance	Cyclic performance	Cell type and performances	Benefits of nanocomposite formation	Ref
$Ti_3C_2T_x$-CNT/PANI	Multi-step synthesis assisted in-situ polymerization strategy	1 M H_2SO_4	1.0 V	429.4 Fg^{-1} @ Current density of 1 Ag^{-1}	93% after 10000 cycles @ 20 Ag^{-1} high current density	-	The ternary nanocomposite electrode displayed improved specific capacitance than that of the components	[98]
Graphene/ $Ti_3C_2T_x$ /PANI	In-situ oxidation copolymeriza-tion of aniline monomers on the surface of $Ti_3C_2T_x$ nanosheets with the decoration of small-sized chem-ical-vapor-de-posited graphene nanosheets	1M H_2SO_4	-0.2 to +0.8 V	452 Fg^{-1}, (volumetric capacitance of 606 Fcm^{-3}) @ current density of 1 Ag^{-1}	72.8% after 5000 cycles @ 10 Ag^{-1} current density	Graphene/$Ti_3C_2T_x$ /PANI//$Ti_3C_2T_x$ asymmetric cell in acid electrolyte, 1.5 V, specific energy of 15.6 and 9.9 $Whkg^{-1}$ @ specific power of 711 and 6347 Wkg^{-1}, respectively	The ternary nanocomposite exhibited the extended discharging period, largest gravimetric and volume specific capacitances than those of $Ti_3C_2T_x$/PANI binary (347 Fg^{-1}, 475 Fcm^{-3}), pristine-$Ti_3C_2T_x$ (109 Fg^{-1}, 281 Fcm^{-3}) electrodes as well as demonstrated enhanced electrochemical stability (80.4% after 5 000 cycles)	[99]
Graphene/ Ti_2CT_x @PANI ternary nanocom-posite	Multi-step chemi-cal synthesis	1 M H_2SO_4	-0.2 to +0.8 V	635 Fg^{-1} (volumetric capacitance of 1143 Fcm^{-3}) @ current density of 1 Ag^{-1}	94.25% after 10000 cycles @ 10 Ag^{-1} current density	Asymmetric cell Graphene/Ti_2CT_x @PANI ternary nanocomposite// graphene, cell voltage of 1.8 V, Specific Energy of 42.3 and 25 $Whkg^{-1}$ @ specific power of 950 and 18000 Wkg^{-1} respectively	The ternary nanocomposite showed better conductivity, electrochemical stability compared to MXenes/ PANI and pristine MXenes electrodes	[100]
PANI@ TiO_2/ $Ti_3C_2T_x$	Hydrothermal treatment com-bined with in-situ polymerization technique	1 M KOH	0.7 V	188.3 Fg^{-1} @ potential sweep rate of 10 mVs^{-1} and 435.4 Fcm^{-2} @ current density of 0.5 Ag^{-1}	94% after 8000 cycles @ 1 Ag^{-1} current density	-	The hierarchical ternary nanocomposite electrode recorded high specific capacitance almost twice greater than that of TiO_2/ $Ti_3C_2T_x$ binary composite electrode in KOH solution.	[102]

3. Conclusion and prospects

Thus, the aforementioned discussion embraces the electrochemical behavior of PANI/MXene nanocomposites obtained from different synthetic procedures, clearly suggesting higher weightage in potential energy storage

applications compared to the constituent materials as well as many others available in the scientific database. Studies revealed that PANI on combining with MXenes have acquired several folds of functional utilities, namely, i) enhanced material processability, ii) improved electronic, structural as well as electrochemical stabilities in various electrolytes, iii) increased electroactive surface density; while PANI has secured MXenes from spontaneous restacking of the layers, thereby improving their electrolyte ion accessibility as well as considerably enhanced the electroactive surface availability in the latter. Besides, MXenes serve as the intrinsic binders for conducting polymer electrodes, readily relaxing the necessity of external electrode-binder addition during device fabrication. Most importantly, their functional versatility lies in the fact that, unlike pristine MXenes that display capacitive behavior in the negative potential range, suitably designed PANI/MXene nanocomposites accomplished impressive capacitive responses in the positive voltage region owing to the distended work function of MXene after composite formation with PANI, thus approving smart designing of advanced asymmetric supercapacitor cells with wider operational voltage window with higher energy and power densities outputs. Besides, considerable progress have been shown by the ternary nanocomposite electrodes with PANI and MXenes as common constituents compared to many other recently developed ternary nanocomposites, particularly, in terms of processing, fabrication cost, device output advantages. Further, the gel-based ternary nanocomposites with these nanomaterials besides securing large areal capacitance and energy density have also proved themselves with appreciable in-vitro and in-vivo biocompatibility benefits that straightway encourage their usages in multifunctional bio-integrative electronics on wet tissues and vital body organ units. Thus, the resultant nanocomposite formation synergistically complements both the electrochemical as well as structural features that judiciously confirm their substantial role in revolutionizing the prevailing supercapacitor technology.

Although this current energy storage material has established a very speedy advancement in a very short time, its relevant findings are still in a very nascent phase. Hence, it is vital to highlight the necessary challenges that ought to be addressed for proper directional progression. Primarily, the achievement of modified composites with upgraded features requires all-round improvement at the individual levels so as to transmit the equivalent benefits in a cooperative manner. Therefore, scheming of both PANI as well as MXenes should not only be restricted to the enhanced specific area, upgraded electronic conductivity, electrochemical and optical behavior, porosity, etc. but also be in their functional assembling and planning, scalability and reproducibility as well. Again, uniform and homogeneous chemical composition in these nanocomposites with all high standards are to be introduced for better demonstrations of characteristic profiles. Further, the fundamental understanding of roles of morphology, surface functionalization, doping effects, bonding interactions at the hybrid phase interfaces, etc., is mandated for attaining detailed insights on their electrochemical energy storage mechanisms. Furthermore, exhaustive studies of the binary and ternary nanocomposite in different electrolytes to optimize both capacitance contributions and high output voltage are yet to be covered. Moreover, different multifunctional features are still to be experimentally explored in a systematic procedure in aid with theoretical research for enlightening their practical ability and commercialization aspects in constructing low pricing, miniature and diligent energy storage devices. Thus, it is quite certain that more exciting and critical progress in this field of MXenes/PANI nanocomposite research remains awaited in the near future.

Acknowledgement

Declaration of interest statement

The author declares no conflict of interest and has received no funding from any sources or organizations for the present project.

References

[1] Jacobson MZ. Review of solutions to global warming, air pollution, and energy security. *Energy and Environmental Science.* 2009; 2(2): 148-173. Available from: https://doi.org/10.1039/b809990c.

[2] Abas N, Kalair A, Khan N. Review of fossil fuels and future energy technologies. *Futures.* 2015; 69: 31-49. Available from: https://doi.org/10.1016/j.futures.2015.03.003.

[3] Dusastre V, Martiradonna L. Materials for sustainable energy. *Nature Materials.* 2017; 16: 15. Available from: https://doi.org/10.1038/nmat4838.

[4] Majumdar D, Ghosh S. Recent advancements of copper oxide based nanomaterials for supercapacitor applications. *Journal of Energy Storage.* 2021; 34: 101995. Available from: https://doi.org/10.1016/j.est.2020.101995.

[5] Majumdar D, Maiyalagan T, Jiang Z. Recent progress in ruthenium oxide-based composites for supercapacitor applications. *ChemElectroChem.* 2019; 6(17): 4343-4372. Available from: https://doi.org/10.1002/celc.201900668.

[6] Majumdar D, Mandal M, Bhattacharya SK. Journey from supercapacitors to supercapatteries: recent advancements in electrochemical energy storage systems. *Emergent Materials.* 2020; 3: 347-367. Available from: https://doi.org/10.1007/s42247-020-00090-5.

[7] Majumdar D. Recent progress in copper sulfide-based nanomaterials for high energy supercapacitor applications. *Journal of Electroanalytical Chemistry.* 2021; 880: 114825. Available from: https://doi.org/10.1016/j.jelechem.2020.114825.

[8] Poonam, Sharma K, Arora A, Tripathi SK. Review of supercapacitors: Materials and devices. *Journal of Energy Storage.* 2019; 21: 801-825. Available from: https://doi.org/10.1016/j.est.2019.01.010.

[9] Teasdale PR. Properties of polyanilines. In: Wallace GG., Sprinks GM., Kane-Maguire LAP, Teasdale PR. (eds.) *Conductive Electroactive Polymers: Intelligent materials Systems.* Taylor & Francis; 2003.

[10] Lee K, Cho S, Park SH, Heeger AJ, Lee CW, Lee SH. Metallic transport in polyaniline. *Nature.* 2006; 441: 65-68. Available from: https://doi.org/10.1038/nature04705.

[11] Genies E, Tsintavis C. Redox mechanism and electrochemical behaviour or polyaniline deposits. *Journal of Electroanalytical Chemistry and Interfacial Electrochemistry.* 1985; 195: 109-128. Available from: https://doi.org/10.1016/0022-0728(85)80009-7.

[12] Fiordiponti P, Pistoia G. An impedance study of polyaniline films in aqueous and organic solutions. *Electrochimica Acta.* 1989; 34(2): 215-221. Available from: https://doi.org/10.1016/0013-4686(89)87088-4.

[13] Conway BE. Transition from "supercapacitor" to "battery" behavior in electrochemical energy storage. *Journal of Electrochemical Society.* 1991; 138: 1539-1548. Available from: http://dx.doi.org/10.1149/1.2085829.

[14] Huang SC, Huang SM, Ng H, Kaner R. Polyaniline capacitors. *Synthetic Metals.* 1993; 57(1): 4047-4052. Available from: https://doi.org/10.1016/0379-6779(93)90555-B.

[15] Rudge A, Raistrick I, Gottesfeld S, Ferraris JP. A study of the electro-chemical properties of conducting polymers for application in electro-chemical capacitors. *Electrochimica Acta.* 1994; 39(2): 273-287. Available from: http://dx.doi.org/10.1016/0013-4686(94)80063-4.

[16] Bandyopadhyay P, Kuila T, Balamurugan J, Nguyen TT, Kim NH, Lee JH. Facile synthesis of novel sulfonated polyaniline functionalized graphene using m-aminobenzene sulfonic acid for asymmetric supercapacitor application. *Chemical Engineering Journal.* 2017; 308: 1174-1184. Available from: https://dx.doi.org/10.1016/j.cej.2016.10.015.

[17] Ryu KS, Wu X, Lee Y, Chang SH. Electrochemical capacitor composed of doped polyaniline and polymer electrolyte membrane. *Journal of Applied Polymer Science.* 2003; 89(5): 1300-1304. Available from: http://dx.doi.org/10.1002/app.12242.

[18] Bian L, Luan F, Liu S, Liu X. Self-doped polyaniline on functionalized carbon cloth as electroactive materials for supercapacitor. *Electrochimica Acta.* 2021; 64: 17-22. Available from: http://dx.doi.org/10.1016/j.electacta.2011.12.012.

[19] Hu C, Chu C. Electrochemical impedance characterization of polyaniline-coated graphite electrodes for electrochemical capacitors deffects of film coverage/thickness and anions. *Journal of Electroanalytical Chemistry.* 2001; 503(1-2): 105-116. Available from: https://dx.doi.org/10.1016/S0022-0728(01)00385-0.

[20] Mu J, Ma G, Peng H, Li J, Sun K, Lei Z. Facile fabrication of self-assembled polyaniline nanotubes doped with d-tartaric acid for high-performance supercapacitors. *Journal of Power Sources.* 2013; 242: 797-802. Available from: https://doi.org/10.1016/j.jpowsour.2013.05.117.

[21] Chen W, Rakhi RB, Alshareef HN. Morphology-dependent enhancement of the pseudocapacitance of template-guided tunable polyaniline nanostructures. *The Journal of Physical Chemistry C.* 2013; 117(29): 15009-15019. Available from: https://doi.org/10.1021/jp405300p.

[22] Wang X, Deng J, Duan X, Liu D, Guo J, Liu P. Crosslinked polyaniline nanorods with improved electrochemical performance as electrode material for supercapacitors. *Journal of Materials Chemistry A*. 2014; 2(31): 12323-12329. Available from: https://doi.org/10.1039/C4TA02231A.

[23] Luo Y, Kong D, Jia Y, Luo J, Lu Y, Zhang D, et al. Self-assembled graphene@PANI nanoworm composites with enhanced supercapacitor performance. *RSC Advances*. 2013; 3: 5851-5859. Available from: https://doi.org/10.1039/C3RA00151B.

[24] Simotwo SK, DelRe C, Kalra V. Supercapacitor electrodes based on high-purity electrospun polyaniline and polyaniline-carbon nanotube nanofibers. *ACS Applied Materials & Interfaces*. 2016; 8: 21261-21269. Available from: https://doi.org/10.1021/acsami.6b03463.

[25] Sivakkumar SR, Kim WJ, Choi JA, MacFarlane DR, Forsyth M, Kim DW. Electrochemical performance of polyaniline nanofibres and polyaniline/multi-walled carbon nanotube composite as an electrode material for aqueous redox supercapacitors. *Journal of Power Sources*. 2007; 171(2): 1062-1068. Available from: https://doi.org/10.1016/j.jpowsour.2007.05.103.

[26] Sharma V, Sahoo A, Sharma Y, Mohanty P. Synthesis of nanoporous hypercrosslinked polyaniline (HCPANI) for gas sorption and electrochemical supercapacitor applications. *RSC Advances*. 2015; 5: 45749-45754. Available from: https://doi.org/10.1039/C5RA03016A.

[27] Mujawar SH, Ambade SB, Battumur T, Ambade RB, Lee S. Electro-polymerization of polyaniline on titanium oxide nanotubes for super-capacitor application. *Electrochimica Acta*. 2011; 56: 4462-4466. Available from: https://doi.org/10.1016/j.electacta.2011.02.043.

[28] Cho S, Shin K, Jang J. Enhanced electrochemical performance of highly porous supercapacitor electrodes based on solution processed polyaniline thin films. *ACS Applied Materials & Interfaces*. 2013; 5: 9186-9193. Available from: https://doi.org/10.1021/am402702y.

[29] Majumdar D. Polyaniline as proficient electrode material for supercapacitor applications: PANI nanocomposites for supercapacitor applications. In: Ramdani N. (ed.) *Polymer Nanocomposites for Advanced Engineering and Military Applications*. IGI Global; 2019. p. 190-219. Available from: https://doi.org/10.4018/978-1-5225-7838-3.ch007.

[30] Majumdar D. Polyaniline nanocomposites: Innovative materials for supercapacitor applications-PANI nanocomposites for supercapacitor applications. In: Ramdani N. (ed.) *Polymer Nanocomposites for Advanced Engineering and Military Applications*. IGI Global; 2019. p. 220-253. Available from: https://doi.org/10.4018/978-1-5225-7838-3.ch008.

[31] Majumdar D. Functionalized-graphene/polyaniline nanocomposites as proficient energy storage material: An overview. *Innovative Energy & Research*. 2016; 5: 145.

[32] Akinwande D, Brennan CJ, Bunch JS, Egberts P, Felts JR, Gao H, et al. A review on mechanics and mechanical properties of 2D materials-Graphene and beyond. *Extreme Mechanics Letters*. 2017; 13: 42-77. Available from: https://doi.org/10.1016/j.eml.2017.01.008.

[33] Zhang H. Ultrathin two-dimensional nanomaterials. *ACS Nano*. 2015; 9: 9451-9469. Available from: https://doi.org/10.1021/acsnano.5b05040.

[34] Natu V, Sokol M, Verger L, Barsoum MW. Effect of edge charges on stability and aggregation of $Ti_3C_2T_z$ MXene Colloidal Suspensions. *The Journal of Physical Chemistry C*. 2018; 122: 27745-27753. Available from: http://dx.doi.org/10.1021/acs.jpcc.8b08860.

[35] Naguib M, Mochalin VN, Barsoum MW, Gogots Y. 25th Anniversary Article: MXenes: A New Family of Two-Dimensional Materials. *Advanced Materials*. 2014; 26: 992-1004. Available from: https://doi.org/10.1002/adma.201304138.

[36] Gogotsi Y, Anasori B. The rise of MXenes. *ACS Nano*. 2019; 13(8): 8491-8494. Available from: https://doi.org/10.1021/acsnano.9b06394.

[37] Naguib M, Kurtoglu M, Presser V, Lu J, Niu J, Heon M, et al. Two-dimensional nanocrystals produced by exfoliation of Ti_3AlC_2. *Advanced Materials*. 2011; 23: 4248-4253. Available from: https://doi.org/10.1002/adma.201102306.

[38] Anasori B, Xie Y, Beidaghi M, Lu J, Hosler BC, Hultman L, et al. Two-dimensional, ordered, double transition metals carbides (MXenes). *ACS Nano*. 2015; 9(10): 9507-9516. Available from: https://doi.org/10.1021/acsnano.5b03591.

[39] Naguib M, Gogotsi Y. Synthesis of two-dimensional materials by selective extraction. *Accounts of Chemical Research*. 2015; 48: 128-135. Available from: https://doi.org/10.1021/ar500346b.

[40] Zhu J, Ha E, Zhao G, Zhou Y, Huang D, Yue G, et al. Recent advance in MXenes: A promising 2D material for catalysis, sensor and chemical adsorption. *Coordination Chemistry Reviews*. 2017; 352: 306-327. Available from: https://doi.org/10.1016/j.ccr.2017.09.012.

[41] Lin SY, Zhang X. Two-dimensional titanium carbide electrode with large mass loading for supercapacitor. *Journal of Power Sources*. 2015; 294: 354-359. Available from: https://doi.org/10.1016/j.jpowsour.2015.06.082.

[42] Yang C, Tang Y, Tian Y, Luo Y, Din MFU, Yin X, et al. Flexible nitrogen-doped 2D titanium carbides (MXene) films constructed by an ex situ solvothermal method with extraordinary volumetric capacitance. *Advanced Energy Materials*. 2018; 8: 1802087. Available from: https://doi.org/10.1002/aenm.201802087.

[43] Yu L, Fan Z, Shao Y, Tian Z, Sun J, Liu Z. Versatile N-doped MXene ink for printed electrochemical energy storage application. *Advanced Energy Materials*. 2019; 9: 1901839. Available from: https://doi.org/10.1002/aenm.201901839.

[44] Wang N, Liu J, Zhao Y, Hu M, Qin R, Shan G. Laser-cutting fabrication of Mxene-based flexible micro-supercapacitors with high areal capacitance. *ChemNanoMat*. 2019; 5: 658. Available from: https://doi.org/10.1002/cnma.201800674.

[45] Zhang C, Kremer MP, Seral-Ascaso A, Park SH, McEvoy N, Anasori B, et al. Stamping of flexible, coplanar micro-supercapacitors using MXene inks. *Advanced Functional Materials*. 2018; 28: 1705506. Available from: https://doi.org/10.1002/adfm.201705506.

[46] Yang W, Yang J, Byun JJ, Moissinac FP, Xu J, Haigh SJ, et al. 3D printing of freestanding MXene architectures for current-collector-free supercapacitors. *Advanced Materials*. 2019; 31: 1902725. Available from: https://doi.org/10.1002/adma.201902725.

[47] Fu Q, Wen J, Zhang N, Wu L, Zhang M, Lin S, et al. Free-standing $Ti_3C_2T_x$ electrode with ultrahigh volumetric capacitance. *RSC Advances*. 2017; 7: 11998-12005. Available from: https://doi.org/10.1039/C7RA00126F.

[48] Ghidiu M, Lukatskaya MR, Zhao MQ, Gogotsi Y, Barsoum MW. Conductive two-dimensional titanium carbide 'clay' with high volumetric capacitance. *Nature*. 2014; 516: 78. Available from: https://doi.org/10.1038/nature13970.

[49] Shang TX, Lin ZF, Qi CS, Liu XC, Li P, Tao Y, et al. 3D macroscopic architectures from self-assembled MXene hydrogels. *Advanced Functional Materials*. 2019; 29: 1903960. Available from: https://doi.org/10.1002/adfm.201903960.

[50] Persson I, el Ghazaly A, Tao Q, Halim J, Kota S, Darakchieva V, et al. Tailoring structure, composition, and energy storage properties of MXenes from selective etching of in-plane, chemically ordered MAX phases. *Small*. 2018; 14: 1703676. Available from: https://doi.org/10.1002/smll.201703676.

[51] Wang Y, Wu Y, Huang Y, Zhang F, Yang X, Ma Y, et al. Preventing graphene sheets from restacking for high-capacitance performance. *The Journal of Physical Chemistry C*. 2011; 115(46): 23192-23197. Available from: https://doi.org/10.1021/jp206444e.

[52] Chen LY, Hou Y, Kang JL, Hirata A, Fujita T, Chen MW. Toward the theoretical capacitance of RuO_2 reinforced by highly conductive nanoporous gold. *Advanced Energy Materials*. 2013; 3(7): 851-856. Available from: https://doi.org/10.1002/aenm.201300024.

[53] Li H, Wang J, Chu Q, Wang Z, Zhang F, Wang S. Theoretical and experimental specific capacitance of polyaniline in sulfuric acid. *Journal of Power Sources*. 2009; 190: 578-586. Available from: https://doi.org/10.1016/j.jpowsour.2009.01.052.

[54] Zhao J, Wu J, Li B, Du W, Huang Q, Zheng M, et al. Facile synthesis of polypyrrole nanowires for high-performance supercapacitor electrode materials. *Progress in Natural Science: Materials International*. 2016; 26: 237-242. Available from: https://doi.org/10.1016/j.pnsc.2016.05.015.

[55] Xie Y, Yang C, Chen P, Yuan D, Guo K. MnO_2-decorated hierarchical porous carbon composites for high-performance asymmetric supercapacitors. *Journal of Power Sources*. 2019; 425: 1-9. Available from: https://doi.org/10.1016/j.jpowsour.2019.03.122.

[56] Guo M, Geng WC, Liu C, Gu J, Zhang Z, Tang Y. Ultrahigh areal capacitance of flexible MXene electrodes: Electrostatic and steric effects of terminations. *Chemistry of Materials*. 2020; 32(19): 8257-8265. Available from: https://doi.org/10.1021/acs.chemmater.0c02026.

[57] Chang L, Stacchiola DJ, Hu YH. An ideal electrode material, 3D surface-microporous graphene for supercapacitors with ultrahigh areal capacitance. *ACS Applied Materials & Interfaces*. 2017; 9(29): 24655-24661. Available from: https://doi.org/10.1021/acsami.7b07381.

[58] Wang QH, Kalantar-Zadeh K, Kis A, Coleman JN, Strano MS. Electronics and optoelectronics of two-dimensional transition metal dichalcogenides. *Nature Nanotechnology*. 2012; 7: 699-712. Available from: https://doi.org/10.1038/nnano.2012.193.

[59] Firestein KL, von Treifeldt JE, Kvashnin DG, Fernando JFS, Zhang C, Kvashnin AG, et al. Young's modulus and tensile strength of Ti_3C_2 MXene nanosheets as revealed by in situ TEM probing, AFM nanomechanical mapping, and theoretical calculations. *Nano Letters*. 2020; 20(8): 5900-5908. Available from: https://doi.org/10.1021/acs.

nanolett.0c01861.

[60] Hu T, Yang J, Li W, Wang X, Li CM. Quantifying the rigidity of 2D carbides (MXenes). *Physical Chemistry Chemical Physics*. 2020; 22: 2115-2121. Available from: https://doi.org/10.1039/C9CP05412J.

[61] Anasori B, Lukatskaya MR, Gogotsi Y. 2D metal carbides and nitrides (MXenes) for energy storage. *Nature Reviews Materials*. 2017; 2: 16098. Available from: https://doi.org/10.1038/natrevmats.2016.98.

[62] Miranda A, Halim J, Lorke A, Barsoum MW. Rendering $Ti_3C_2T_x$(MXene) monolayers visible. *Materials Research Letters*. 2017; 5: 322-328. Available from: https://doi.org/10.1080/21663831.2017.1280707.

[63] Ibragimova R, Erhart P, Rinke P, Komsa H-P. Surface functionalization of 2D MXenes: Trends in distribution, composition, and electronic properties. *Journal of Physical Chemistry Letters*. 2021; 12(9): 2377-2384. Available from: https://doi.org/10.1021/acs.jpclett.0c03710.

[64] Shao Y, Zhang F, Shi X, Pan H. N-Functionalized MXenes: ultrahigh carrier mobility and multifunctional properties. *Physical Chemistry Chemical Physics*. 2017; 19: 28710-28717. Available from: https://doi.org/10.1039/C7CP05816K.

[65] Xie Y, Dall'Agnese Y, Naguib M, Gogotsi Y, Barsoum MW, Zhuang HL, et al. Prediction and characterization of MXene nanosheet anodes for non-lithium-ion batteries. *ACS Nano*. 2014; 8: 9606-9615. Available from: https://doi.org/10.1021/nn503921j.

[66] Peng J, Chen X, Ong W-J, Zhao X, Li N. Surface and heterointerface engineering of 2D MXenes and their nanocomposites: Insights into electro-and photocatalysis. *Chem*. 2019; 5(1): 18-50. Available from: https://doi.org/10.1016/j.chempr.2018.08.037.

[67] Aghaei SM, Torres I, Baboukani AR, Khakpour I, Wang C. Impact of surface oxidation on the structural, electronic transport, and optical properties of two-dimensional titanium nitride (Ti_3N_2) MXene. *Computational Condensed Matter*. 2019; 20: e00382. Available from: https://doi.org/10.1016/j.cocom.2019.e00382.

[68] Ronchi RM, Arantes JT, Santos SF. Synthesis, structure, properties and applications of MXenes: Current status and perspectives. *Ceramics International*. 2019; 45: 18167-18188. Available from: https://doi.org/10.1016/j.ceramint.2019.06.114.

[69] Xiong D, Li X, Bai Z, Lu S. Recent advances in layered $Ti_3C_2T_x$ MXene for electrochemical energy storage. *Small*. 2018; 14: 1703419. Available from: https://doi.org/10.1002/smll.201703419.

[70] Lukatskaya MR, Bak SM, Yu X, Yang XQ, Barsoum MW, Gogotsi Y. Probing the mechanism of high capacitance in 2D titanium carbide using in situ X-ray absorption spectroscopy. *Advanced Energy Materials*. 2015; 5: 1500589. Available from: https://doi.org/10.1002/aenm.201500589.

[71] Hu M, Li Z, Hu T, Zhu S, Zhang C, Wang X. High-capacitance mechanism for $Ti_3C_2T_x$ MXene by in situ electrochemical raman spectroscopy investigation. *ACS Nano*. 2016; 10: 11344-11350. Available from: https://doi.org/10.1021/acsnano.6b06597.

[72] Li J, Yuan X, Lin C, Yang Y, Xu L, Du X, et al. Achieving high pseudocapacitance of 2D titanium carbide (MXene) by cation intercalation and surface modification. *Advanced Energy Materials*. 2017; 7: 1602725. Available from: https://doi.org/10.1002/aenm.201602725.

[73] Lukatskaya MR, Kota S, Lin Z, Zhao M, Shpigel N, Levi MD, et al. Ultra high-rate pseudocapacitive energy storage in two-dimensional transition metal carbides. *Nature Energy*. 2017; 2: 17105. Available from: https://doi.org/10.1038/nenergy.2017.105.

[74] Kayali E, Vahidmohammadi A, Orangi J, Beidaghi M. Controlling the dimensions of 2D MXenes for ultrahigh-rate pseudocapacitive energy storage. *ACS Applied Materials & Interfaces*. 2018; 10: 25949-25954. Available from: https://doi.org/10.1021/acsami.8b07397.

[75] Zhan C, Naguib M, Lukatskaya M, Kent PRC, Gogotsi Y, Jiang D. Understanding the MXene pseudocapacitance. *Journal of Physical Chemistry Letters*. 2018; 9: 1223-1228. Available from: https://doi.org/10.1021/acs.jpclett.8b00200.

[76] Wu W, Wang C, Zhao C, Wei D, Zhu J, Xu Y. Facile strategy of hollow polyaniline nanotubes supported on Ti_3C_2-MXene nanosheets for High-performance symmetric supercapacitors. *Journal of Colloid and Interface Science*. 2020; 580: 601-613. Available from: https://doi.org/10.1016/j.jcis.2020.07.052.

[77] Vahid MA, Moncada J, Chen H, Kayali E, Orangi J, Carrero CA, et al. Thick and freestanding MXene/PANI pseudocapacitive electrodes with ultrahigh specific capacitance. *Journal of Materials Chemistry A*. 2018; 6(44): 22123-22133. Available from: https://doi.org/10.1039/C8TA05807E.

[78] Wu W, Niu D, Zhu J, Gao Y, Wei D, Liu X, et al. Organ-like Ti_3C_2 Mxenes/polyaniline composites by chemical grafting as high-performance supercapacitors. *Journal of Electroanalytical Chemistry*. 2019; 847: 113203. Available from: https://doi.org/10.1016/j.jelechem.2019.113203.

[79] Wang Y, Wang X, Li X, Bai Y, Xiao H, Liu Y, et al. Scalable fabrication of polyaniline nanodots decorated MXene

film electrodes enabled by viscous functional inks for high-energy-density asymmetric supercapacitors. *Chemical Engineering Journal.* 2021; 405: 126664. Available from: https://doi.org/10.1016/j.cej.2020.126664.

[80] Xu H, Zheng D, Liu F, Li W, Lin J. Synthesis of an MXene/polyaniline composite with excellent electrochemical properties. *Journal of Materials Chemistry A.* 2020; 8(12): 5853-5858. Available from: https://doi.org/10.1039/D0TA00572J.

[81] Li Y, Kamdem P, Jin XJ. Hierarchical architecture of MXene/PANI hybrid electrode for advanced asymmetric supercapacitors. *Journal of Alloys and Compounds.* 2021; 850: 156608. Available from: https://doi.org/10.1016/j.jallcom.2020.156608.

[82] Ren Y, Zhu J, Wang L, Liu H, Liu Y, Wu W, et al. Synthesis of polyaniline nanoparticles deposited on two-dimensional titanium carbide for high-performance supercapacitors. *Materials Letters.* 2018; 214: 84-87. Available from: https://doi.org/10.1016/j.matlet.2017.11.060.

[83] Chen B, Song Q, Zhou Z, Lu C. A novel sandwiched porous MXene/polyaniline nanofibers composite film for high capacitance supercapacitor electrode. *Advanced Materials Interfaces.* 2021; 8(12): 2002168. Available from: https://doi.org/10.1002/admi.202002168.

[84] Li K, Wang X, Li S, Urbankowski P, Li J, Xu Y, et al. An ultrafast conducting polymer@MXene positive electrode with high volumetric capacitance for advanced asymmetric supercapacitors. *Small.* 2020; 16(4): 1906851. Available from: https://doi.org/10.1002/smll.201906851.

[85] Neampet S, Ruecha N, Qin J, Wonsawat W, Chailapakul O, Rodthongkum N. A nanocomposite prepared from platinum particles, polyaniline and aTi$_3$C$_2$ MXene for amperometric sensing of hydrogen peroxide and lactate. *Microchimica Acta.* 2019; 186(12): 752. Available from: https://doi.org/10.1007/s00604-019-3845-3.

[86] Yin G, Wang Y, Wang W, Qu Z, Yu D. A flexible electromagnetic interference shielding fabric prepared by construction of PANI/MXene conductive network via layer-by-layer assembly. *Advanced Materials Interfaces.* 2021; 8(6): 2001893. Available from: https://doi.org/10.1002/admi.202001893.

[87] Boota M, Jung E, Ahuja R, Hussain T. MXene binder stabilizes pseudocapacitance of conducting polymers. *Journal of Materials Chemistry A.* 2021; 9: 20356. Available from: https://doi.org/10.1039/D1TA05861D.

[88] Chen Z, Wang Y, Han J, Wang T, Leng Y, Wang Y, et al. Preparation of polyaniline onto DL-tartaric acid assembled MXene surface as an electrode material for supercapacitors. *ACS Applied Energy Materials.* 2020; 3(9): 9326-3648. Available from: https://doi.org/10.1021/acsaem.0c01662.

[89] Li P, Jin Z, Peng L, Zhao F, Xiao D, Jin Y, et al. Stretchable all-gel-state fiber shaped supercapacitors enabled by macromolecularly interconnected 3D graphene/nanostructured conductive polymer hydrogels. *Advanced Materials.* 2018; 30: 1800124. Available from: https://doi.org/10.1002/adma.201800124.

[90] Wei H, Dong J, Fang X, Zheng W, Sun Y, Qian Y, et al. Ti$_3$C$_2$T$_x$ MXene/polyaniline (PANI) sandwich intercalation structure composites constructed for microwave absorption. *Composites Science and Technology.* 2018; 169: 52-59. Available from: https://doi.org/10.1016/j.compscitech.2018.10.016.

[91] Dong Y, Guan S, Zhou X, Chang Q, Jiang G. Co-intercalation of CTAB favors the preparation of Ti$_3$C$_2$T$_x$/PANI composite with improved electrochemical performance. *Ionics.* 2021; 27(6): 2501-2508. Available from: https://https://doi.org/10.1007/s11581-021-04025-w.

[92] Wang L, Tan Y, Yu Z, Tian H, Lai Y, He Y, et al. Three-dimensional polyaniline architecture enabled by hydroxyl-terminated Ti$_3$C$_2$T$_x$ MXene for high-performance supercapacitor electrodes. *Materials Chemistry Frontiers.* 2021; 5: 7883-7891. Available from: https://doi.org/10.1039/D1QM01059J.

[93] Wang Y, Wang X, Li X, Bai Y, Xiao H, Liu Y, et al. Scalable fabrication of polyaniline nanodots decorated MXene film electrodes enabled by viscous functional inks for high-energy-density asymmetric supercapacitors. *Chemical Engineering Journal.* 2021; 405: 126664. Available from: https://doi.org/10.1016/j.cej.2020.126664.

[94] Zhou J, Kang Q, Xu S, Li X, Liu C, Ni L, et al. Ultrahigh rate capability of 1D/2D polyaniline/titanium carbide (MXene) nanohybrid for advanced asymmetric supercapacitors. *Nano Research.* 2022; 15: 285-295. Available from: https://doi.org/10.1007/s12274-021-3472-2.

[95] Wang L, Tan Y, Yu Z, Tian H, Lai Y, He Y, et al. In situ polymerized polyaniline/MXene (V$_2$C) as building blocks of supercapacitor and ammonia sensor self-powered by electromagnetic-triboelectric hybrid generator. *Materials Chemistry Frontiers.* 2021; 88: 106242. Available from: https://doi.org/10.1016/j.nanoen.2021.106242.

[96] Yun J, Echols I, Flouda P, Wang S, Easley A, Zhao X, et al. Layer-by-layer assembly of polyaniline nanofiber and MXene thin film electrodes for electrochemical energy storage. *ACS Applied Materials & Interfaces.* 2019; 11(51): 47929-47938. Available from: https://doi.org/10.1021/acsami.9b16692.

[97] Majumdar D. Review on current progress of MnO$_2$-based ternary nanocomposites for supercapacitor applications. *ChemElectroChem.* 2021; 8(2): 291-336. Available from: https://doi.org/10.1002/celc.202001371.

[98] Cai YZ, Fang YS, Cao WQ, He P, Cao MS. MXene-CNT/PANI ternary material with excellent supercapacitive

performance driven by synergy. *Journal of Alloys and Compounds*. 2021; 868: 159159. Available from: https://doi.org/10.1016/j.jallcom.2021.159159.

[99] Wang S, Ma Z, Lü Q-F, Yang H. Two-dimensional $Ti_3C_2T_x$/polyaniline nanocomposite from the decoration of small-sized graphene nanosheets: Promoted pseudocapacitive electrode performance for supercapacitors. *ChemElectroChem.* 2019; 6 (10): 2748-2754. Available from: https://doi.org/10.1002/celc.201900433.

[100] Fu J, Yun J, Wu S, Li L, Yu L, Kim KH. Architecturally robust graphene-encapsulated MXene Ti_2CT_x@polyaniline composite for high-performance pouch-type asymmetric supercapacitor. *ACS Applied Materials & Interfaces.* 2018; 10(40): 34212-34221. Available from: https://doi.org/10.1021/acsami.8b10195.

[101] Liu Y, Zhou H, Zhou W, Meng S, Qi C, Liu Z, et al. Biocompatible, high-performance, wet-adhesive, stretchable all-hydrogel supercapacitor implant based on PANI@rGO/Mxenes electrode and hydrogel electrolyte. *Advanced Energy Materials*. 2021; 11(30): 2101329. Available from: https://doi.org/10.1002/aenm.202101329.

[102] Lu X, Zhu J, Wu W, Zhang B. Hierarchical architecture of PANI@TiO_2/$Ti_3C_2T_x$ ternary composite electrode for enhanced electrochemical performance. *Electrochimica Acta*. 2017; 228: 282-289. Available from: https://doi.org/10.1016/j.electacta.2017.01.025.

[103] Wei Y, Luo W, Zhuang Z. Dai B, Ding J, Li T, et al. Fabrication of ternary MXene/MnO_2/polyaniline nanostructure with good electrochemical performances. *Advanced Composites and Hybrid Materials*. 2021. Available from: https://doi.org/10.1007/s42114-021-00323-z.